Department of Physics, Engineering Physics & Astronomy

PHYS 455 - Engineering Physics Design Project

Design and Control of a Double Inverted Pendulum

Authors:
Beattie, W.
Esche, M.
Fox, A.
Georgas, P.
Simpson, J.

Submitted To:
Dr. J. Morelli
Dr. K. Robbie

April 12th, 2010

We would like to extend our gratitude towards Chuck Hearns, Gary Contant, Steve Gillen, Bernie Ziomkowitz, Abdol-Reza Mansouri, and our TA Greg Demand. This project would not have been possible without their patience and help.

Abstract

This report constitutes the culmination of a multi-month design project to design and stabilize a double-inverted pendulum system. We begin by motivating the problem and presenting the mathematical the theoretical tools needed to achieve the goal. The mechanical, electrical, and software design components are outlined, along with the relevant safety protocols. We describe the characterization of our set-up, present results, and put forward recommendations for future work.

Contents

1 Introduction, Motivation & Objectives

The Double Inverted Pendulum (DIP) control problem is a natural extension of the classical inverted pendulum scenario. Such systems have been thoroughly investigated in the literature, and typically involve an actuated cart or mobile platform constrained to move in one dimension. A freely swinging pendulum link is attached to the cart, with a second freely swinging pendulum attached to the end of the first pendulum such that the motion of both pendulums is confined to a single plane in line with the motion of the cart. This setup is displayed in Figure 1 below.

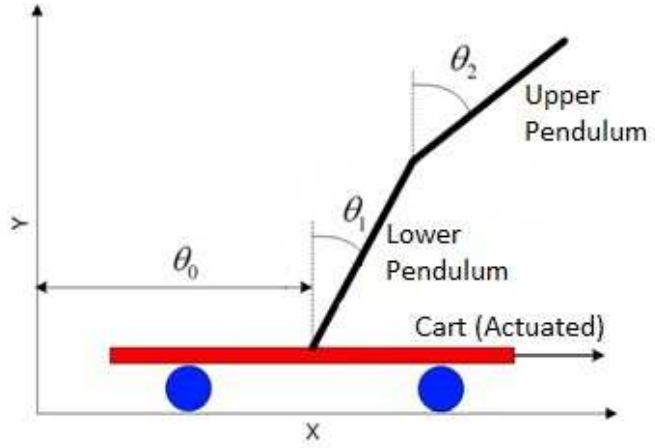

Figure 1: Typical double inverted pendulum system

The underactuated DIP system is commonly used as a benchmark and testing ground for control algorithms due to its highly unstable internal dynamics. The primary objective of this project was to stabilize the DIP system shown in Figure 1 about its upward, unstable equilibrium position. This was accomplished using a closed loop control algorithm with first and second joint angles and cart position as inputs and the force applied to the actuated cart as the output. In other words, the motion of the cart is used to control the angle and motion of the lower pendulum such that control of the upper pendulum can be achieved by further motion of the cart. The specifics of the control algorithm are discussed in Section 3.

1. The closed loop system should be stable about the fully upright equilibrium position.
2. The steady state error in the angles of each pendulum joint should be zero within the accuracy of the measurement device.
3. The step response of the cart position to a setpoint of 30 cm from the zero position should have a settling time of less than 10 seconds.
4. The overshoot of the cart position step response should not be greater than 20% of the value of the step.

2 Modeling

A schematic of mechanical system is depicted in Figure 1. The mathematical modeling of this system is unpleasant to display and can be found in Appendix D. Although we do not explicitly develop the analogous equations for a single inverted pendulum on a cart in this report, they follow from a similar procedure, and are ubiquitous in the mechanics and control literature [Bradshaw, 1996].

3 Control Theory

We again refer the reader primarily to Appendix D for a detailed account of the control theoretical ideas required for stabilization of this system. After consulting in person with Professor Mansouri, a control theorist in the Math department, the group decided to use a full-state observer for velocity estimation as opposed to a filtering or finite-difference system. Here however, we primarily discuss design issues. There are several procedural methods for placing the poles of state space systems. Here we will consider the use of the *Linear Quadratic Regulator* (LQR) method [Astrom, 2008]. In this method, one supplies *relative weights* of how important the control of each state variable is, and an algorithm is then applied to calculate the necessary K matrix. This procedure (and indeed, controller design in general) necessarily generates engineering trade-offs. In our case, we wish to sacrifice cart position in exchange for angular stability.

The reader is referred to [Astrom, 2008] or [Lewis, 2003] for more control theoretic ideas, and to [Khan et al., 2009], [Wang et al., 2010], or [Bradshaw, 1996] for inverted pendulum details.

4 Apparatus

4.1 General Description

The apparatus consists primarily of a mechanical robot and electronics which power the robot and communicate with the computer. Shown below in Figure 2 is an block diagram showing the operation of the apparatus as it was used during the testing. An image of the apparatus is shown in Figure 13 in the appendix. The double pendulum was actuated by a rotational motor, coupled to a timing belt. The motor was powered using a bipolar operational amplifier (BOP) which receives a control signal from MATLAB software on a desktop personal computer. Additionally, the joint angles were measured using rotational potentiometers. A third potentiometer was coupled to the axle of the motor, which allows information on the position of the cart to be fed back to the computer. A power supply

was used in order to ensure a consistent and repeatable reference voltage in day to day operation of the potentiometers. Finally, a third voltage source was required to power the safety switch circuit which required a relay.

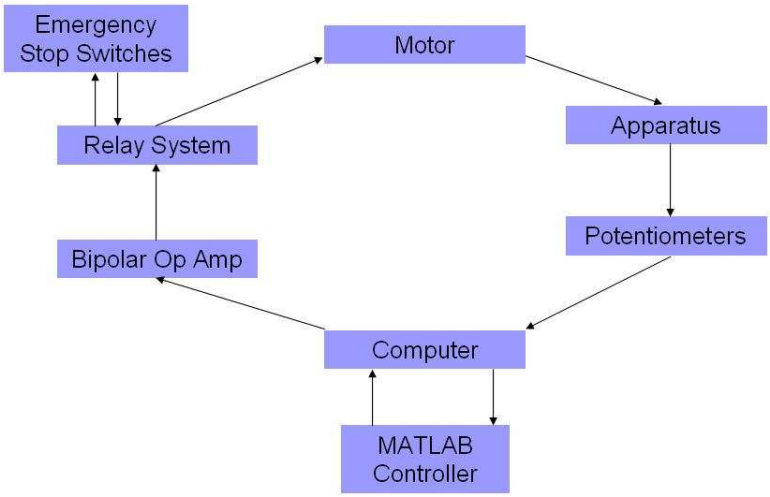

Figure 2: Block diagram for the operation of the apparatus

4.2 Mechanical Design

The first major design decision that was made was how the cart would be controlled. Several options, such as driving the cart with an on-board motor, driving the cart with a stationary motor at one end and a timing belt, or using a rotating arm under the small angle regime. The latter option was the most logical choice for a few reasons. Primarily the mass of the cart could be greatly reduced by avoiding having to move the motor. The rotating arm was also undesirable since the arc through which the cart could travel and stay in the linear regime was relatively small. The problem becomes much harder if the nonlinear regime is considered. Having settled on a cart and timing belt, the next step was to design a track to which the cart would be paired. It was felt necessary to purchase a track and cart system in order to ensure the quality and therefore repeatability of what was considered the part which required the most precision. With cost and size in mind, a cart and track pair were purchased, as shown in the appendix in Figure 14.

The next design consideration was the timing belt. Several factors led to the choice to use the helical timing belt shown in Figure 15. Normal rubber timing belts are subject to slipping and with rapid changes in motor direction often undergo tensions which distort the belt and compromise its integrity. The helical timing belt performs with less slip and far less distortion, performance criteria that are critical to the functioning of the apparatus. Additionally, a tensioning gear was used to both avoid the obstruction of the cart with the timing belt passing over it as well as to vary the tension to find the optimal operating conditions.

In order to obtain feedback from the apparatus, transducers had to be implemented which performed different roles. The three outputs required were the position of the cart on the track and the angles of both links with respect to the previous link. While options such as ultrasonic position transducers and optical encoders were available to use, due to the ease of use, cost, and availability rotary potentiometers were used. They have three leads, two of which are connected to a reference voltage and the third is a voltage linearly proportional to angular deviation. These provided 0.25 of accuracy, limited only by the ability of the analog to digital converted we used.

The motor was selected as a recommendation from Professor Andrew Lewis, who has had experience with motors for control labs run in the applied mathematics department.

For physical properties of the links (i.e. mass, moment of inertia, dimensions) and mechanical drawings of designed parts, see the appendix.

4.3 Electrical Design

A safety relay circuit was designed by that would kill power to the motor if the cart was near the end of the track, or could by triggered manually. A relay was employed because the motor draws a lot of current and the circuit only requires a small current to function, contributing to the safety. The relay was powered by a voltage source.

In addition, a bipolar operational amplifier (BOP) was used to power the motor. A small control signal could be output from MATLAB, and the BOP amplified the signal to proved ample amperage to drive the motor. Finally another voltage source was used as the reference voltage for the potentiometers.

4.4 Software Design

Matlab code was written to implement both the simulation and real time control of the system. This code makes explicit use of the fast matrix multiplication available in Matlab, and the real-time portion was coded to be as fast as possible to ensure no significant delay in the control system. A sampling rate of approximately 250 Hz was achieved. It should be noted that this in itself constitutes an engineering tradeoff, as a light-weight integration code was selected over a more serious Runge-Kutta style algorithm.

5 Safety & Finances

The hazards associated with this experiment were mitigated through the use of hardware, software and safety protocols. The two primary hazards were electric shock from the high

currents required to drive the DC motor which actuates the cart and impact from the moving pendulum links.

In terms of hardware, to prevent electric shock the electrical components connected to the motor were insulated and the apparatus itself was grounded. To prevent impact with the pendulum, padded end stops were placed at the ends of the track to contain the cart and prevent damage which could cause erratic behaviour. To keep the motor from running the cart into these end stops, switches tripped by the cart were placed by the ends of the track. These were part of a relay circuit that cut power to the motor when a switch was tripped. This circuit also included two manual switches to both restore and cut motor power. A circuit diagram is included in Appendix A. The control program also included conditions which would stop the motor when the pendulum fell or when the cart reached an end stop. A padded stick was used to manually stop the pendulum from swinging once it had fallen and the apparatus was placed in an area that minimized access, preventing injury.

In addition to these safety features, a set of protocols was created and posted around the apparatus. The full protocols are included in Appendix C. The purpose of these protocols was to minimize the risk to the operators of the apparatus.

The project was constrained to a budget of $500. While most of the experimental apparatus was borrowed or machined several components were purchased from online suppliers. Expenditure details are shown in Figure 3 below. Original invoices for these orders are available from science stores.

Item	Supplier	Description	Part Number	DOP	Cost (CAD)
Guide Rail (1)	McMaster Carr	1 m anodized aluminum	9867K12	02/02/2010	105
Guide Block (1)	McMaster Carr	Teflon coated sliding block	9867K2	02/02/2010	60
‘1/4 Bearing (1)	McMaster Carr	Fixed mount bearing	5912K1	02/02/2010	10
Rotary Pot (1)	Digikey	5.0 kΩ continuous turn	SP132C-5.0K-ND	01/04/2010	36
Rotary Pot (1)	Digikey	2.0 kΩ continuous turn	SP132C-2.0K-ND	01/04/2010	36
Total (tax and shipping not included)					247

Figure 3: Project budget breakdown

The components above were purchased due to time constraints, lack of available equipment and lack of machining expertise. Precise mechanical components were required to ensure agreement between the modeled dynamics and the actual dynamics. The small active range of joint angles required highly linear potentiometers to ensure measurement accuracy.

6 Experimentation & Characterization

A number of experiments were performed to characterize and parameterize the system and its performance.

The moving components (the cart, links, attached components) needed to have their masses, lengths, and moments of inertia characterized. The masses and lengths were trivial measurements while the moments of inertia where determined by timing the period length of small angle oscillations and substituting the value into the following formula which also adjusts for the point of rotation

$$I = \frac{T^2 mgl}{4\pi^2} - ml^2. \tag{1}$$

Another important consideration was determining whether the friction associated with the track was viscous or Coulombic friction as it would effect the derivation of the equations as well as the type of coefficient used. Experiments were performed by lifting the track and plotting the position as a function of time and it was determined that dry friction was the main source from the track. An appropriate static friction coefficient was determined while the kinetic friction coefficient is taken into account in the following voltage to force calibration.

The most important calibration was to determine how what force on the cart would result from the varying control voltage output by the computer. After initial testing to determine appropriate amplification levels, an experiment was performed to determine the control voltage to force calibration. This was done by placing the cart on one side of the track and applying a constant control voltage to have the motor move the cart from one side to the other. This was repeated in both directions for varying control voltages. The position of the cart was then plotted against time and doubly differentiated to acquire the acceleration, or equivalently by knowing the mass of the components, the force. The results of this experiment are shown in Figure 4. As one can see there is a significant dead zone for which the control voltage does not cause the motor to operate. Also, the calibrations are different in the two different directions which is logical due to the asymmetry of the apparatus setup.

7 Results & Analysis

The behaviour of the SIP and DIP were recorded through state measurements. The SIP was of secondary focus and the results are presented in Appendix A accordingly. Figure 5 below shows the behaviour of the DIP for a 30cm step response. The simulated result is shown in Figure 6 below.

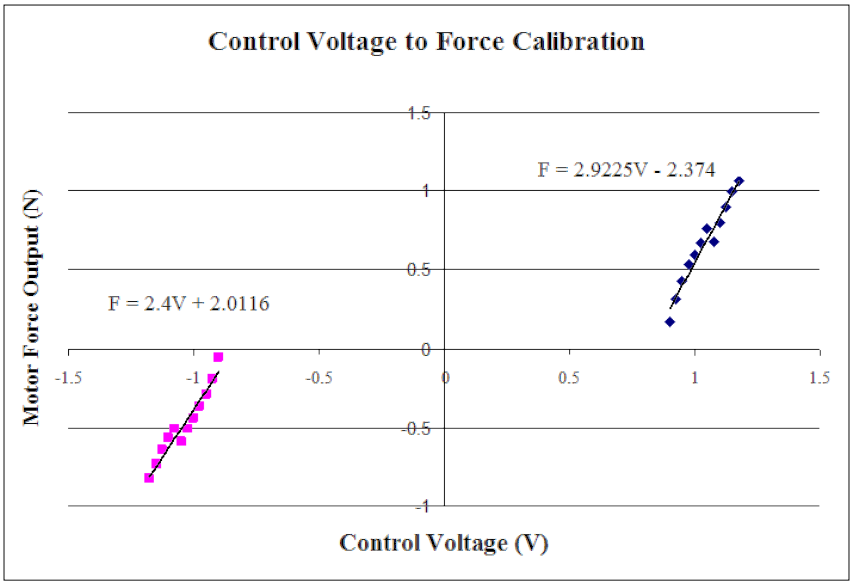

Figure 4: Calibration of the Control Voltage to the Output Motor Force

An immediate qualitative observation is the correlation between θ_1 and θ_2. The controller works to force the two angles in phase. This behaviour is observed in the simulation as well. This can be understood by considering the requirements for translation. If the two angles were out of phase trying to move the pendulum would cause the links to fold at the second joint. An overshoot of 37.8 cm was observed. System memory was exhausted before stable oscillations could be reached but the settling time is greater than 30 s. In contrast simulation of the same controller under an identical step response yields an overshoot of 5.5 cm and a settling time of 5.2 s. The difference between simulation and results is very large and is discussed in further detail in Appendix A with the SIP results. Given the instability of the equilibrium, small errors in measurement and output can result in large instabilities.

8 Discussion & Recommendations

The successes and failures attributable to the project are easily identifiable. The controls developed by the team were certainly adequate and sophisticated enough to achieve stability in the double inverted pendulum system. The difficulty in the problem results from inherent problems with modeling any dynamic system. Some factors are not fully accounted for, and this requires extensive tuning of the system in almost all circumstances.

The biggest problem encountered by the team was the behavior of the cart and track system. It was felt that these parts would be too difficult to machine, and thus they were purchased under the assumption that they would behave ideally. Due to budget constraints, a track and cart were selected that moved by sliding rather than rolling. The

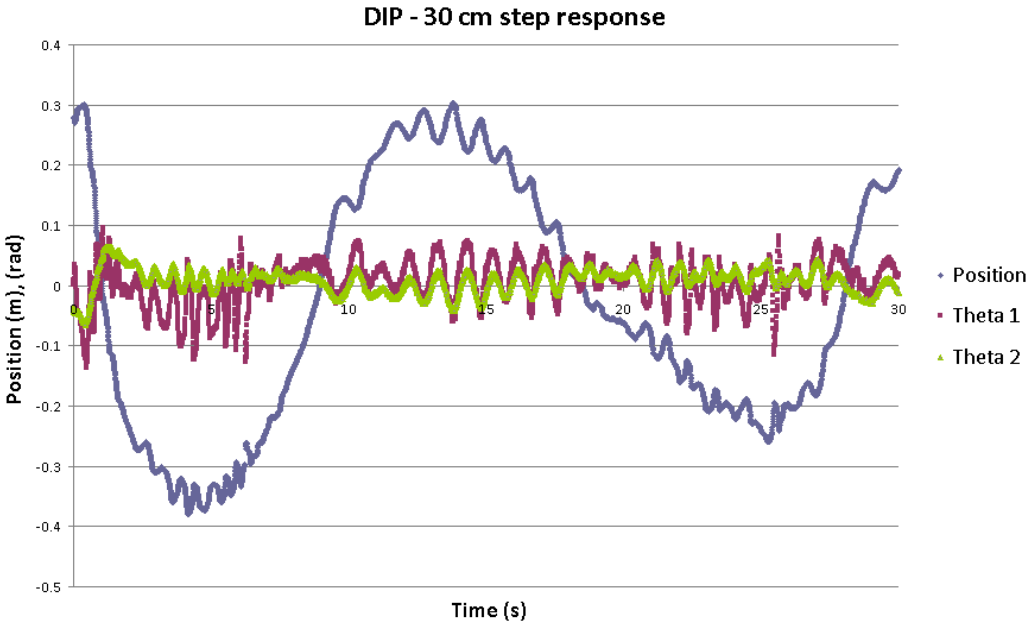

Figure 5: DIP step response experimental performance. Initial conditions x=27.9 cm, ?1 = 0.01 rad, ?2 = -0.04 rad. Gains used: Ke=[0.18,-1,2,0.15,0.06,0.2628,0.01]*50 . The system is stable to the step but equilibrium oscillations were not reached before system memory was exhausted.

effect was that the cart did not pair ideally to the cart. This meant that the friction profile on the track was not only irregular but occasionally random, since the cart occasionally would bite the track and therefore not respond to the input signals.

Thus, improvements in the experimental apparatus would begin with replacing the track and cart system with a rolling cart. This should lead to not only less friction, but a much more uniform friction along the whole of the track. This would greatly simplify the dynamic modeling and the control system could be reevaluated with this better apparatus.

9 Conclusions

The report details each element of the DIP design process. Concept formulation, system modeling, apparatus and design, controller synthesis, experimentation and analysis were all explored by the group. Results from model simulations were used to drive the design parameters for the mechanical system and actuators. The controller was designed to minimize steady state oscillations and to produce the best possible step response characteristics. Safety concerns were met with appropriate protocol and redundant forms of emergency stops. The system was constructed and assembled by the group in the lab

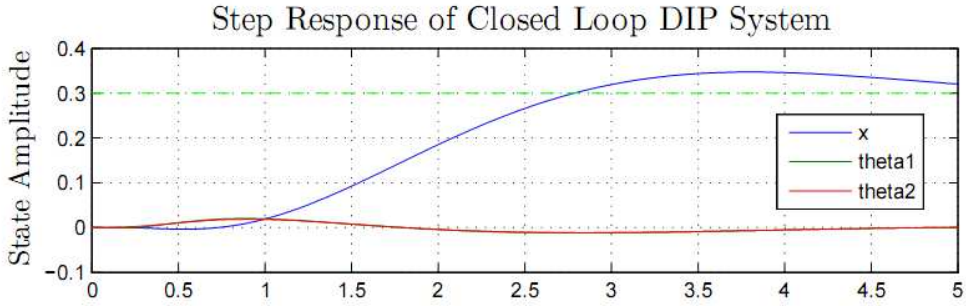

Figure 6: Step response of the DIP Gains used: Ke=[0.18,-1,2,0.15,0.06,0.2628,0.01]*50.

setting with minimal additional purchases required. The completed apparatus was characterized by a set of mini-experiments to measure needed parameters and tune the model.

Ultimately a design was reached that satisfied the budget, time, and stability constraints of the project but failed to meet the settling time and overshoot objectives initially laid out. The best DIP 30 cm step response achieved a 37.8 cm overshoot and a settling time of over 30 s, greater than the initial goal of 6 cm and 10 s. The results obtained were not consistent with the predictions from simulation due to measurement error and unmodeled system dynamics. The group believes that further refinements of mechanical components and tuning of the controller could improve the performance characteristics of the DIP to within the target range. Further problems like swing up or stabilization of other unstable DIP equilibrium remain as more difficult challenges for future work.

10 Appendix A - Detailed Results

As an intermediate step in stabilizing the DIP the group ran a set of experiments on the SIP using a similar controller. The results of varying step responses in position and link angle are shown in Figure 7 and Figure 8 below

Step (cm)	Overshoot (cm)	Settling Time (s)	SS Oscillation Amplitude (cm)	SS Oscillation Amplitude (rad)	Max Cart Velocity (m/s)	Max Link Velocity (rad/s)
0	1.6	1.68	6.00	0.035	0.21	3.37
10.81	4.4	2.96	6.00	0.035	0.95	3.67
20.08	3.6	5.416	6.00	0.035	0.52	4.46
30.58	6.36	7.67	6.00	0.035	0.52	3.76
32.77	7.94	8.09	6.00	0.035	0.78	2.07
34.4	FAILURE	FAILURE	FAILURE	FAILURE	FAILURE	FAILURE

Figure 7: Response of the SIP to a variety of angular steps. Response parameters for each trial are recorded in the table. The final step resulted in failure to stabilize

Step (deg)	Overshoot (cm)	Settling Time (s)	SS Oscillation Amplitude (cm)	SS Oscillation Amplitude (rad)	Max Cart Velocity (m/s)	Max Link Velocity (rad/s)
5.21	1.6	4.22	6.00	0.035	0.16	0.14
7.39	2.4	3.27	6.00	0.035	0.87	3.68
12.72	9.9	4.34	6.00	0.035	1.27	4.77
18.68	14.5	5.90	6.00	0.035	1.43	4.53
21.03	27.1	5.24	6.00	0.035	1.77	4.67
24.47	FAILURE	FAILURE	FAILURE	FAILURE	FAILURE	FAILURE

Figure 8: Response of the SIP to a variety of angular steps. Response parameters for each trial are recorded in the table. The final step resulted in failure to stabilize

No step responses achieved absolute convergence to equilibrium as expected, but instead oscillated about 6 cm. Trends in the step response data show increasing convergence time and overshoot with increasing step magnitude. A range of stabilizable steps is also established. The system is found to converge for position steps of 33 cm and 22^o. The SIP simulations predict a stability range of 29 cm and 17^o.

Substantial disagreement was observed between simulation and measurement in the DIP. Measurement and output error are likely sources of the disagreement. This effect can be studied by examining simulation results of the SIP with and without error. Figure 9 shows the expected behaviour of the SIP when subject to white measurement noise. Figure 10 shows the expected behaviour of the SIP when subject to a zero position calibration error.

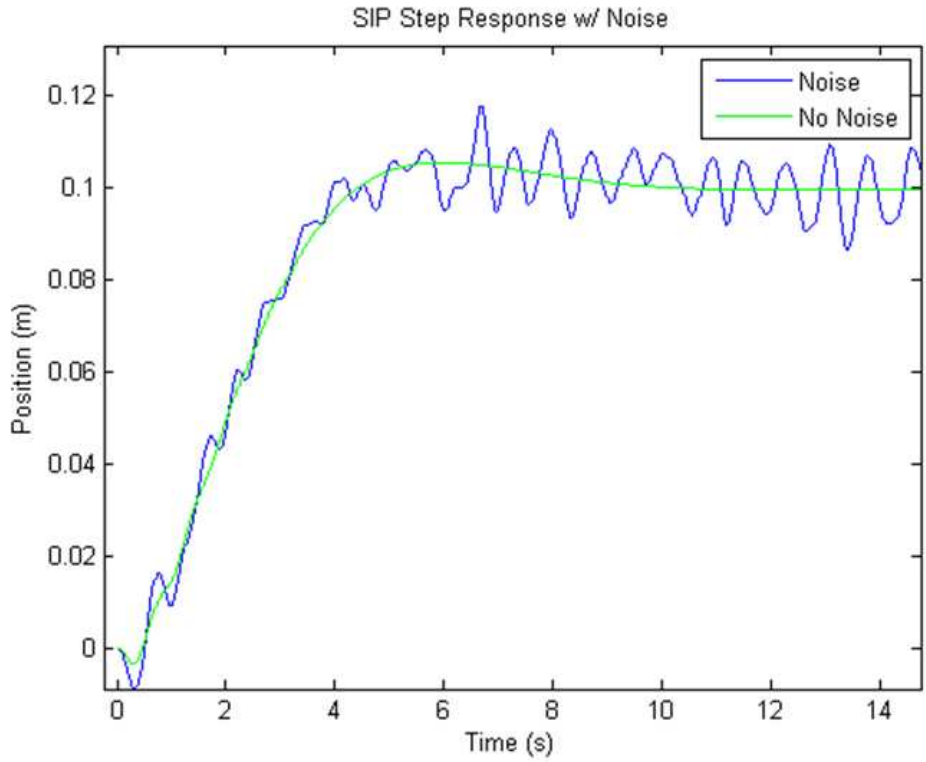

Figure 9: Simulated response of the SIP to a 10 cm step. Angle and position measurements are subjected to a white noise with standard deviations of 0.50 and 3 cm

While the offset does not produce the steady state oscillations observed in practise the white noise on measurement does produce a pattern consistent with the behaviour seen in lab. Figure 11 shows the measured data for a 10.8 cm step below for comparison.

The magnitude of oscillations seen in practise is greater than those seen in simulation for generous measurement errors. Inconsistencies in the track and motor, while difficult to quantify or estimate, also contribute to steady state oscillations and can be used to explain the discrepancy.

11 Appendix B - Additional Design Pictures

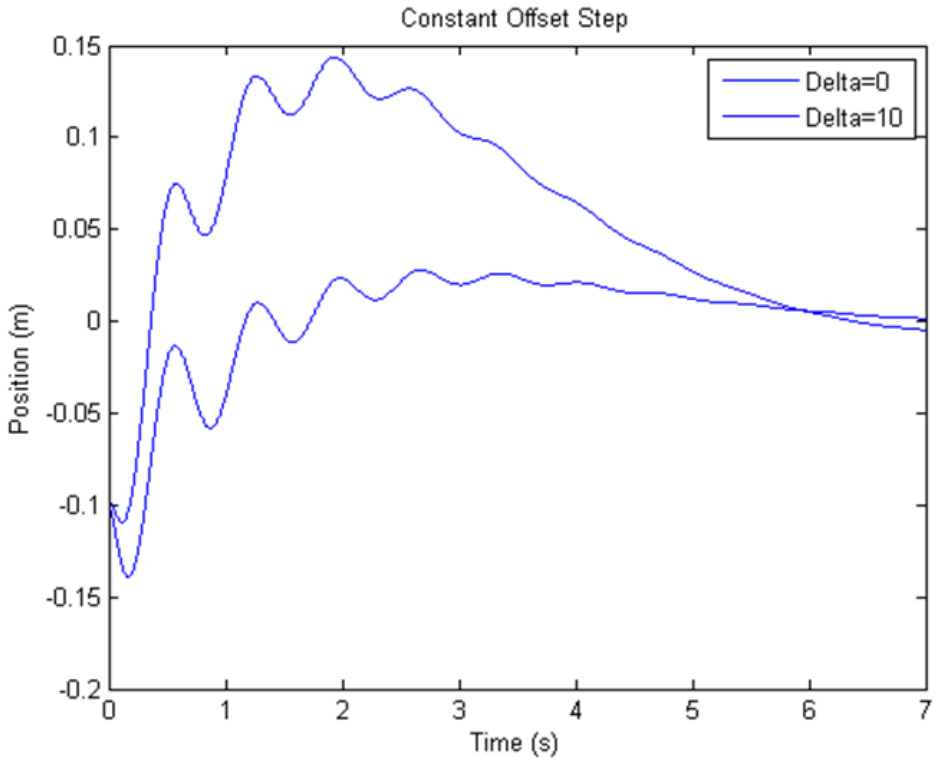

Figure 10: Simulated response of the SIP to a 10 cm step. The angle measurement is subject to a hard offset of 100

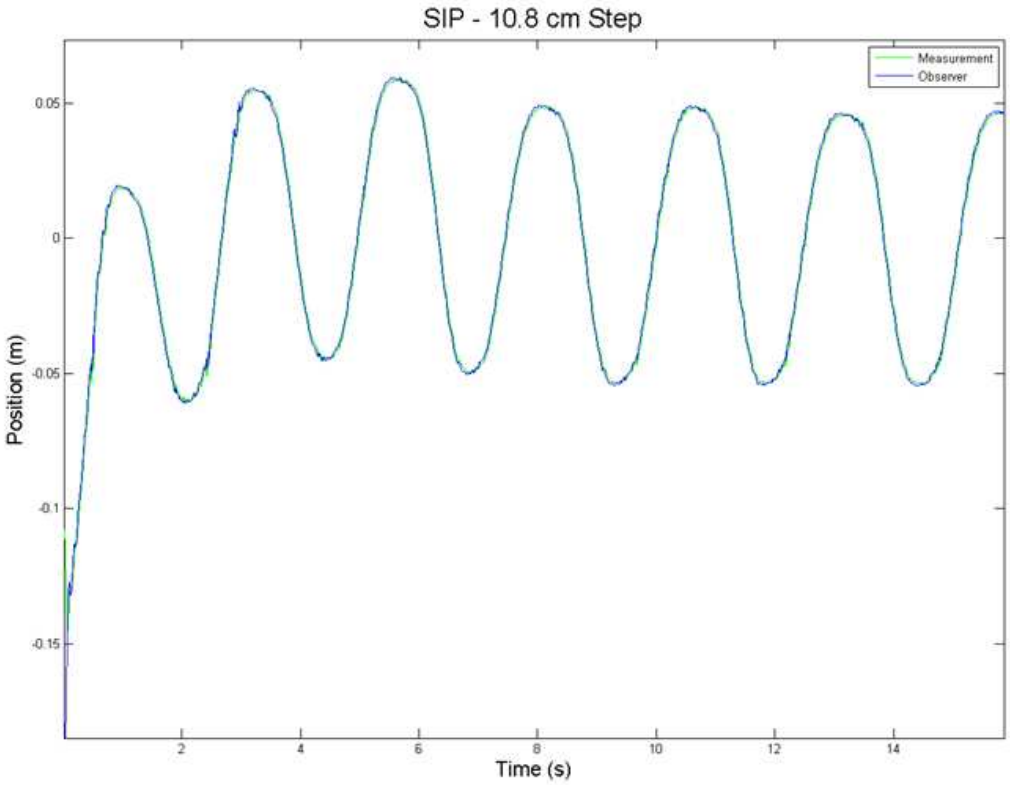

Figure 11: Response of the SIP to a 10.8 cm step. Steady state oscillations of 6cm are observed

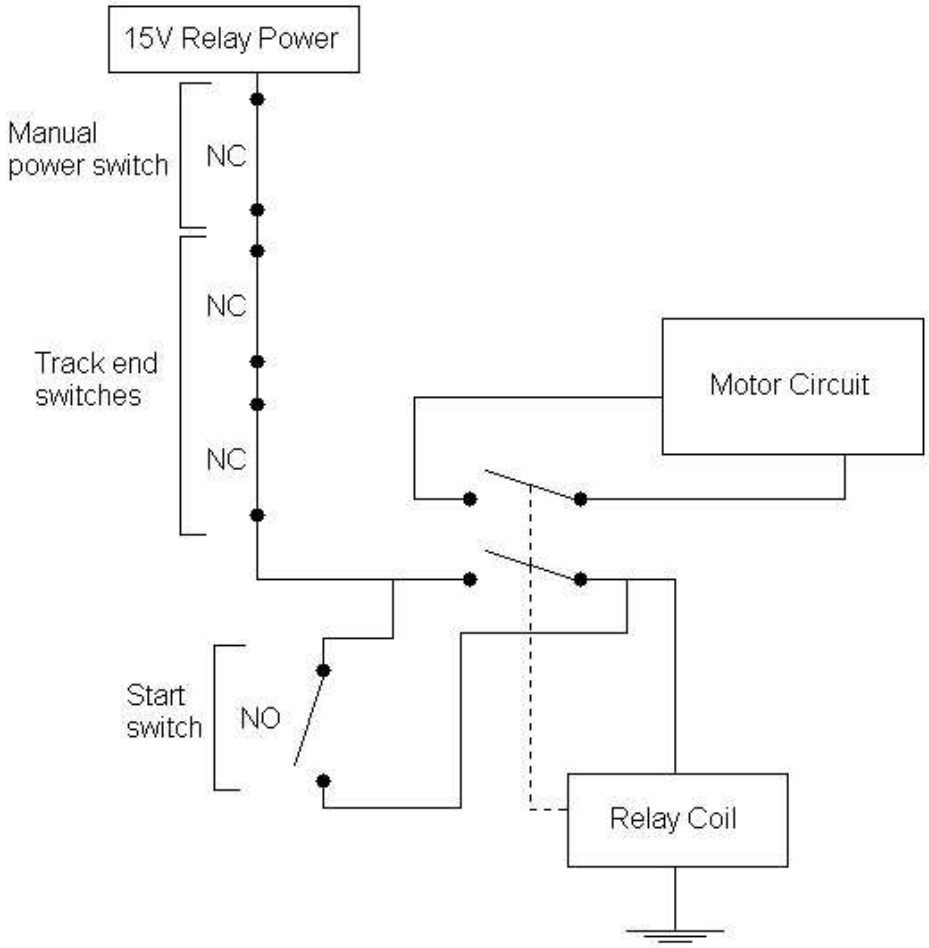

Figure 12: Relay circuit to interrupt motor power

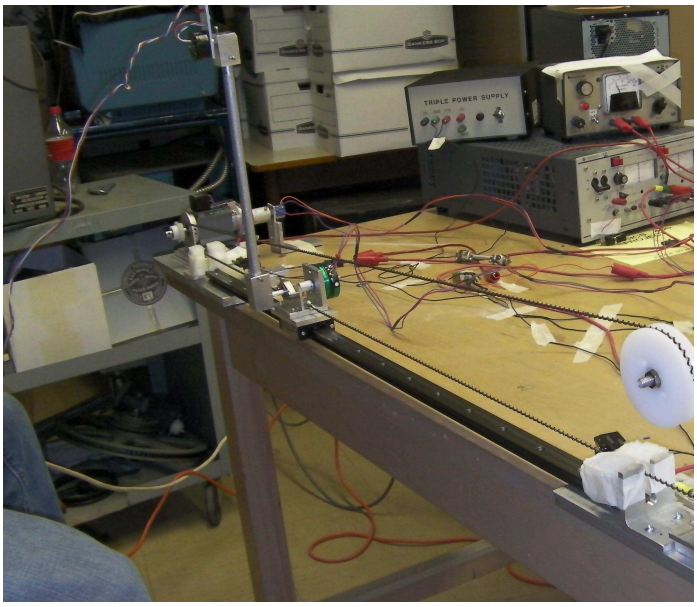

Figure 13: The experimental apparatus in functioning form with the double pendulum linkages

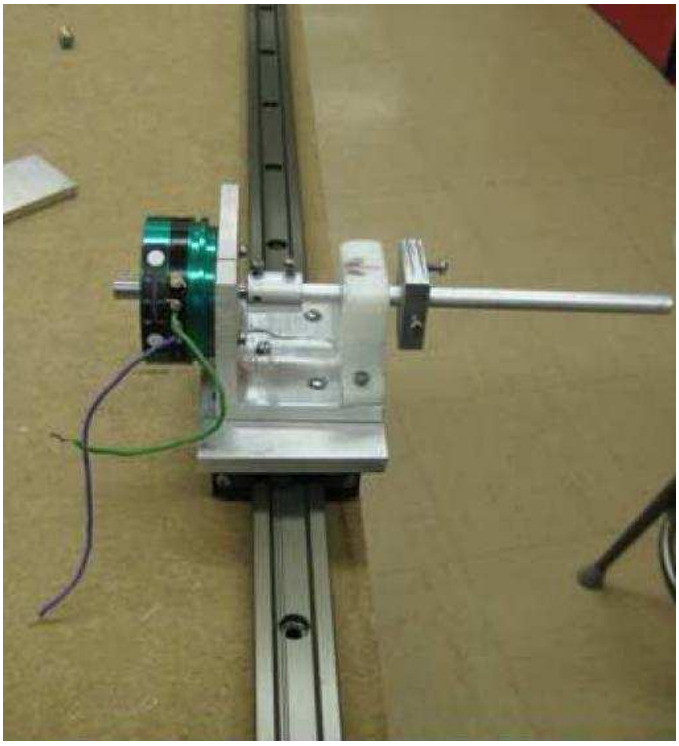

Figure 14: The track and cart pair used in experimental apparatus

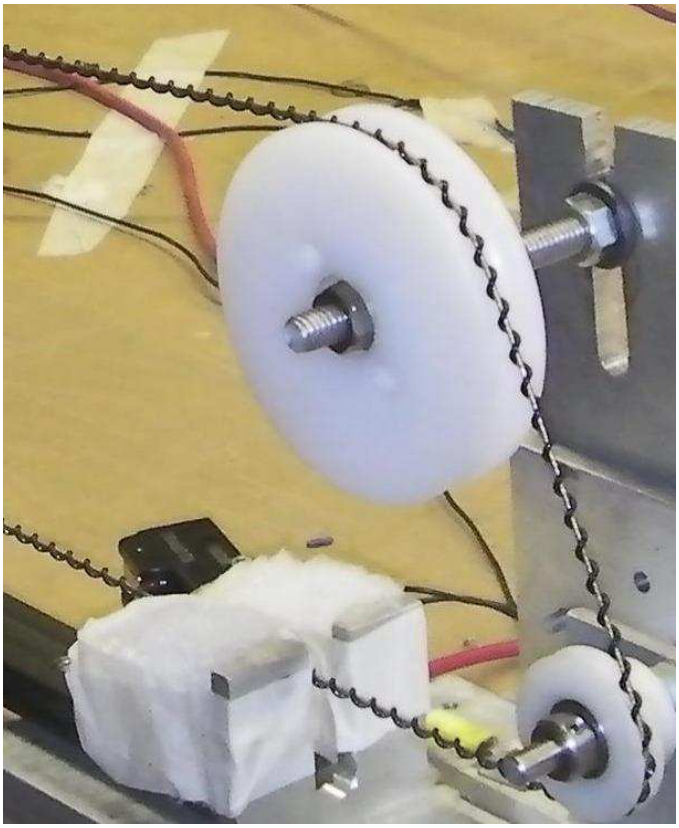

Figure 15: The helical timing belt used to translate the rotational motion of the motor to the translational motion of the cart

12 Appendix B2 - Mechanical Drawings

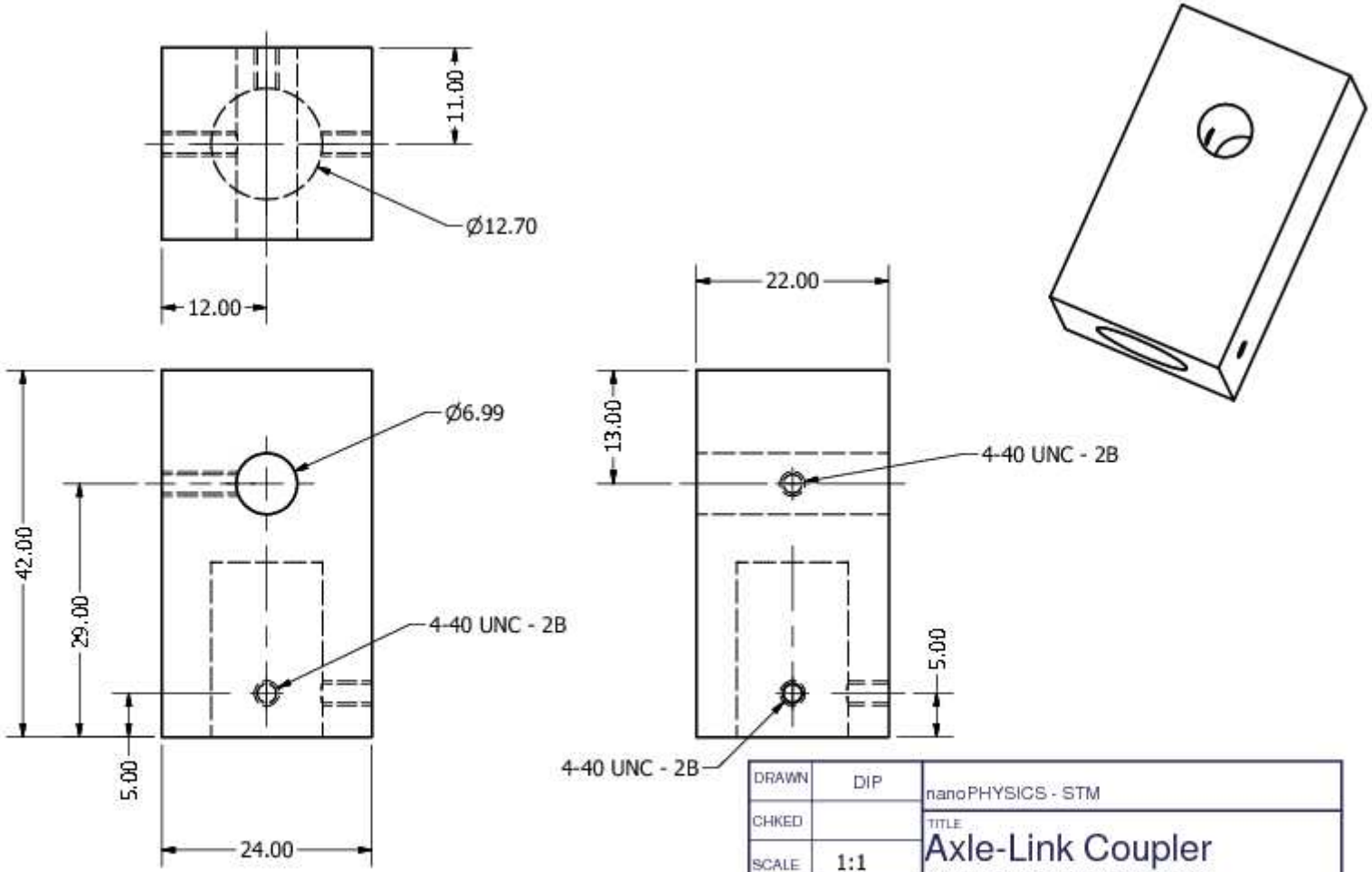

DRAWN	DIP
CHKED	
SCALE	1:1
UNITS	mm
DATE	12/04/2010

nanoPHYSICS - STM

TITLE

Axle-Link Coupler

E:\Documents and Settings\nanoPhysics\My Documents\Inventor\Pendulum\AxleLink Coupler.ipt

UNLESS SPECIFIED:

.X	±0.25
.XX	±0.15
.XXX	±0.03
ANG	± 1°

DWG NO AxleLink Coupler

REV

MODEL: E:\Documents and Settings\nanoPhysics\My Documents\Inventor\Pendulum\AxleLink Coupler.ipt

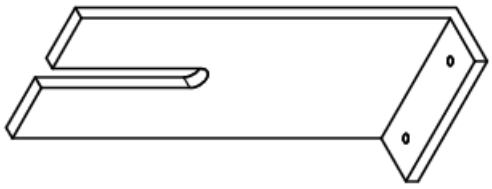

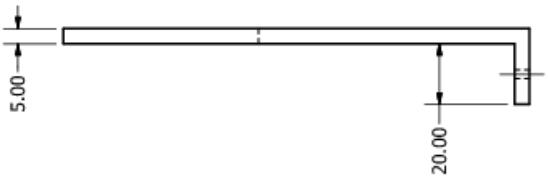

DRAWN	DIP	nanoPHYSICS - STM	
CHKED		TITLE: Tension Cog Stand	
SCALE	1:1	C:\Documents and Settings\nanoPhysics\My Documents\Inventor\Pendulum\Tension Cog Stand.idw	
UNITS	mm	SPECIFIED: X ±0.25 XX ±0.15 XXX ±0.03 ANG ±1°	
DATE	12/04/2010	DWG NO Tension Cog Stand	REV
		MODEL: C:\Documents and Settings\nanoPhysics\My Documents\Inventor\Pendulum\Tension Cog Stand.ipt	

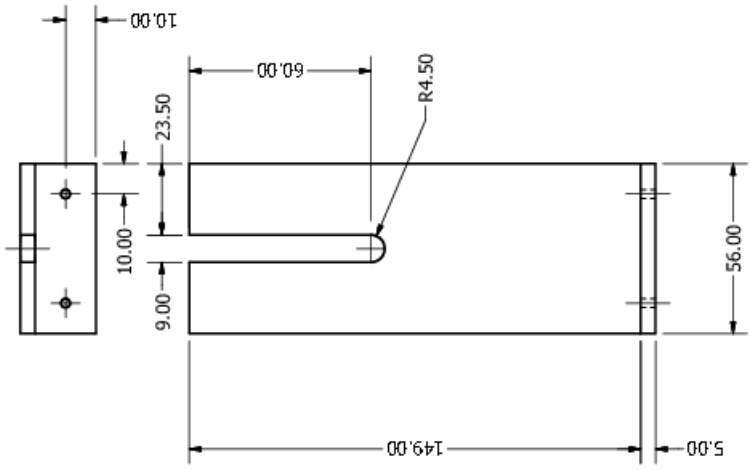

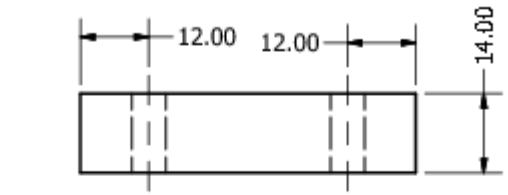

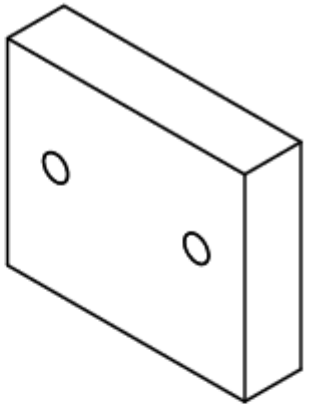

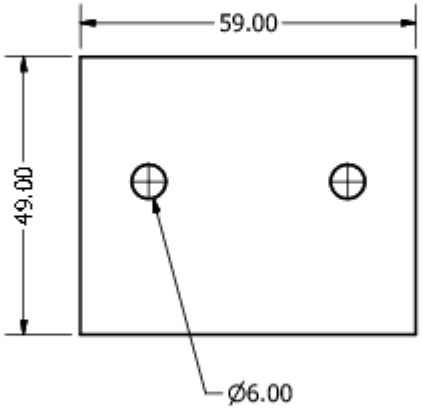

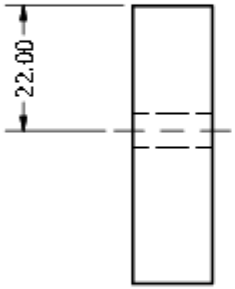

DRAWN	DIP	nanoPHYSICS - STM
CHKED		TITLE: Cog Spacer
SCALE	1:1	E:\Documents and Settings\nanoPhysics\My Documents\Inventor\Pendulum\Cog Spacer.idw
UNITS	mm	FINISH
DATE	12/04/2010	DWG NO: Cog Spacer
		REV

SPECIFIED:
.X ±0.25
.XX ±0.15
.XXX ±0.03
ANG ± 1°

MODEL: E:\Documents and Settings\nanoPhysics\My Documents\Inventor\Pendulum\Cog Spacer.ipt

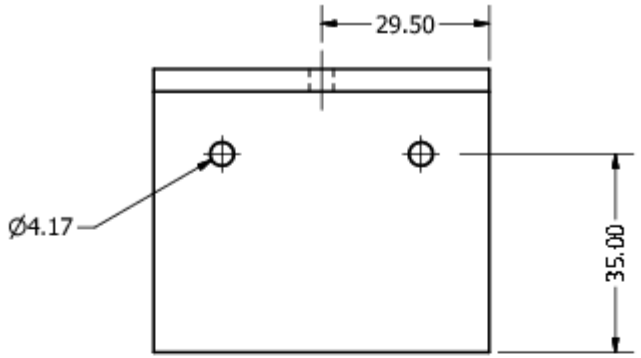

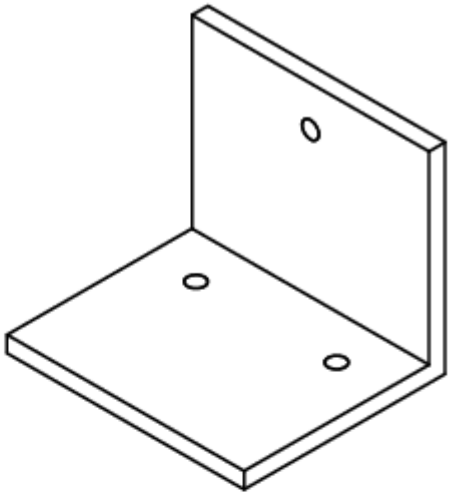

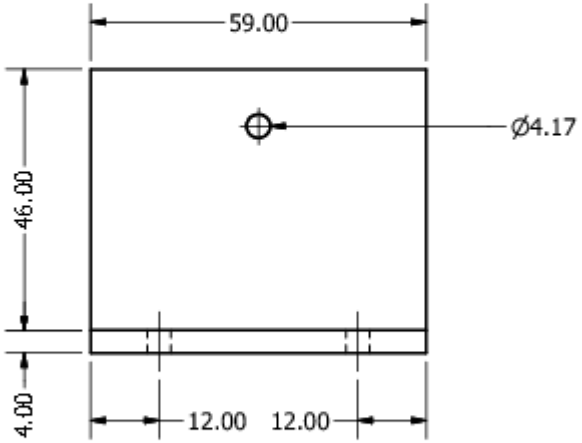

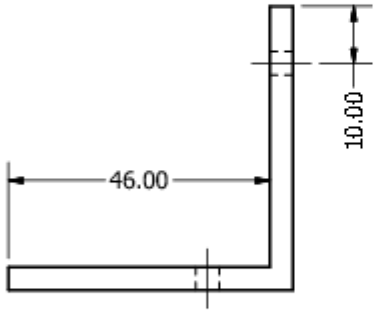

DRAWN	DIP	nanoPHYSICS - STM
CHKED		TITLE: End Cog Holder
SCALE	1:1	E:\Documents and Settings\nanoPhysics\My
UNITS	mm	SIZE: A3
DATE	12/04/2010	DWG NO: End Cog Holder
		REV

UNLESS OTHERWISE SPECIFIED:
.X ±0.25
.XX ±0.15
.XXX ±0.03
ANG ± 1°

MODEL : E:\Documents and Settings\nanoPhysics\My Documents\Inventor\Pendulum\End Cog Holder.ipt

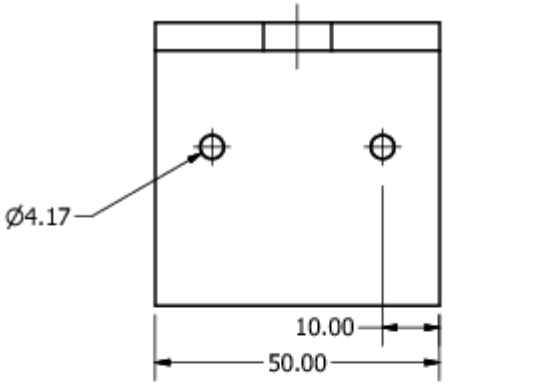

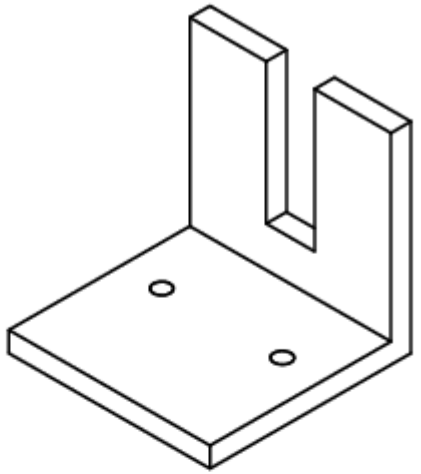

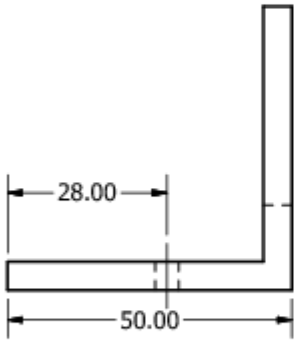

DRAWN	DIP	nanoPHYSICS - STM
CHKED		TITLE: Safety Stop
SCALE	1:1	E:\Documents and Settings\nanoPhysics\My Documents\Inventor\Pendulum\Safety Stop.ipt
UNITS	mm	FINISH
DATE	12/04/2010	SPECIFIED: .X ±0.25, .XX ±0.15, .XXX ±0.03, ANG ± 1°
		DWG NO: Safety Stop; REV

MODEL: E:\Documents and Settings\nanoPhysics\My Documents\Inventor\Pendulum\Safety Stop.ipt

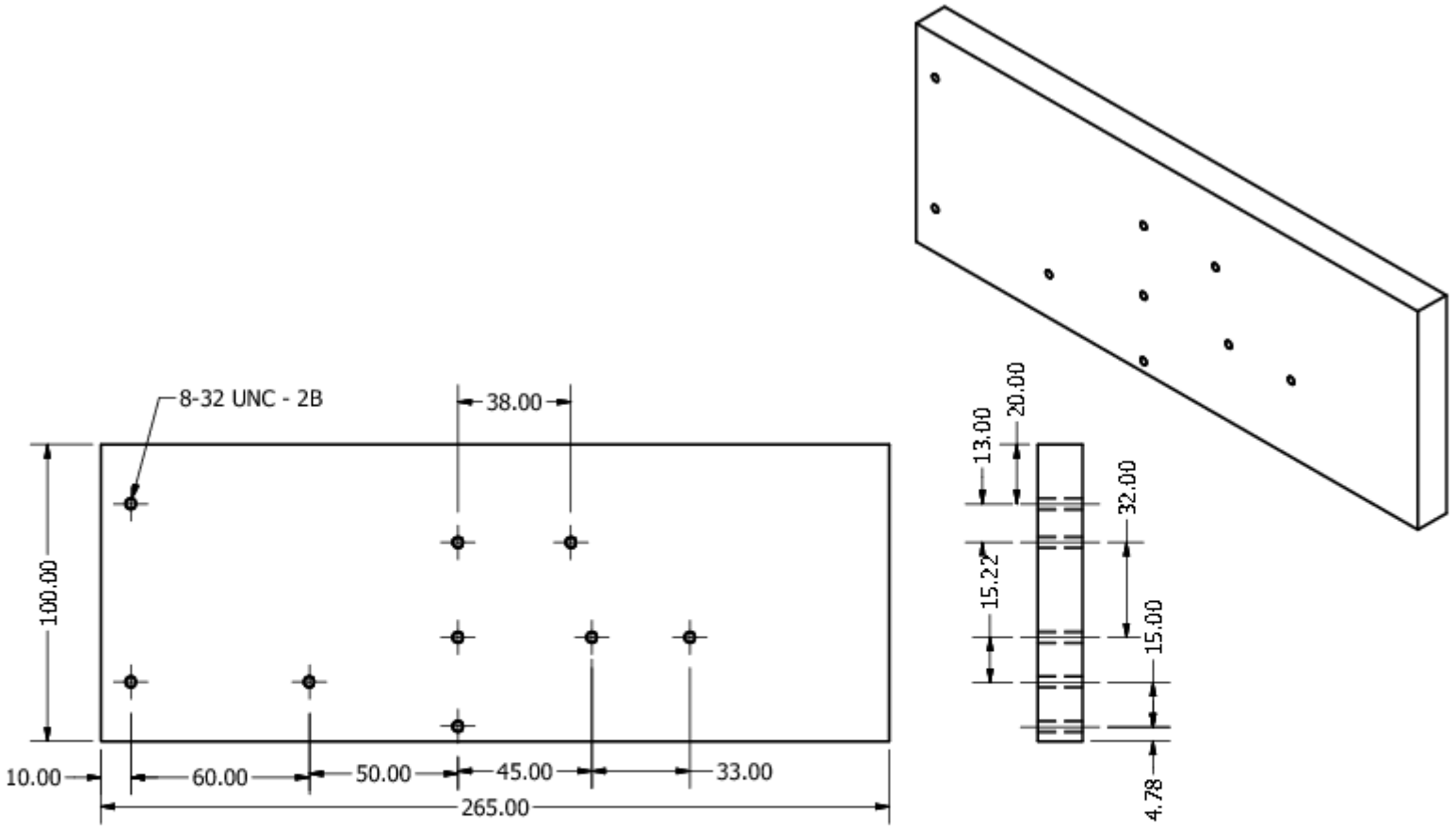

DRAWN	DIP
CHKED	
SCALE	1:1
UNITS	mm
DATE	12/04/2010

nanoPHYSICS - STM

TITLE

Cog Side End Piece

E:\Documents and Settings\nanoPhysics\My Documents\Inventor\Pendulum\Cog Side Base Plate.idw

SPECIFIED:

.X ±0.25
.XX ±0.15
.XXX ±0.03
ANG ± 1°

DWG NO Cog Side Base Plate

REV

MODEL: E:\Documents and Settings\nanoPhysics\My Documents\Inventor\Pendulum\Cog Side Base Plate.ipt

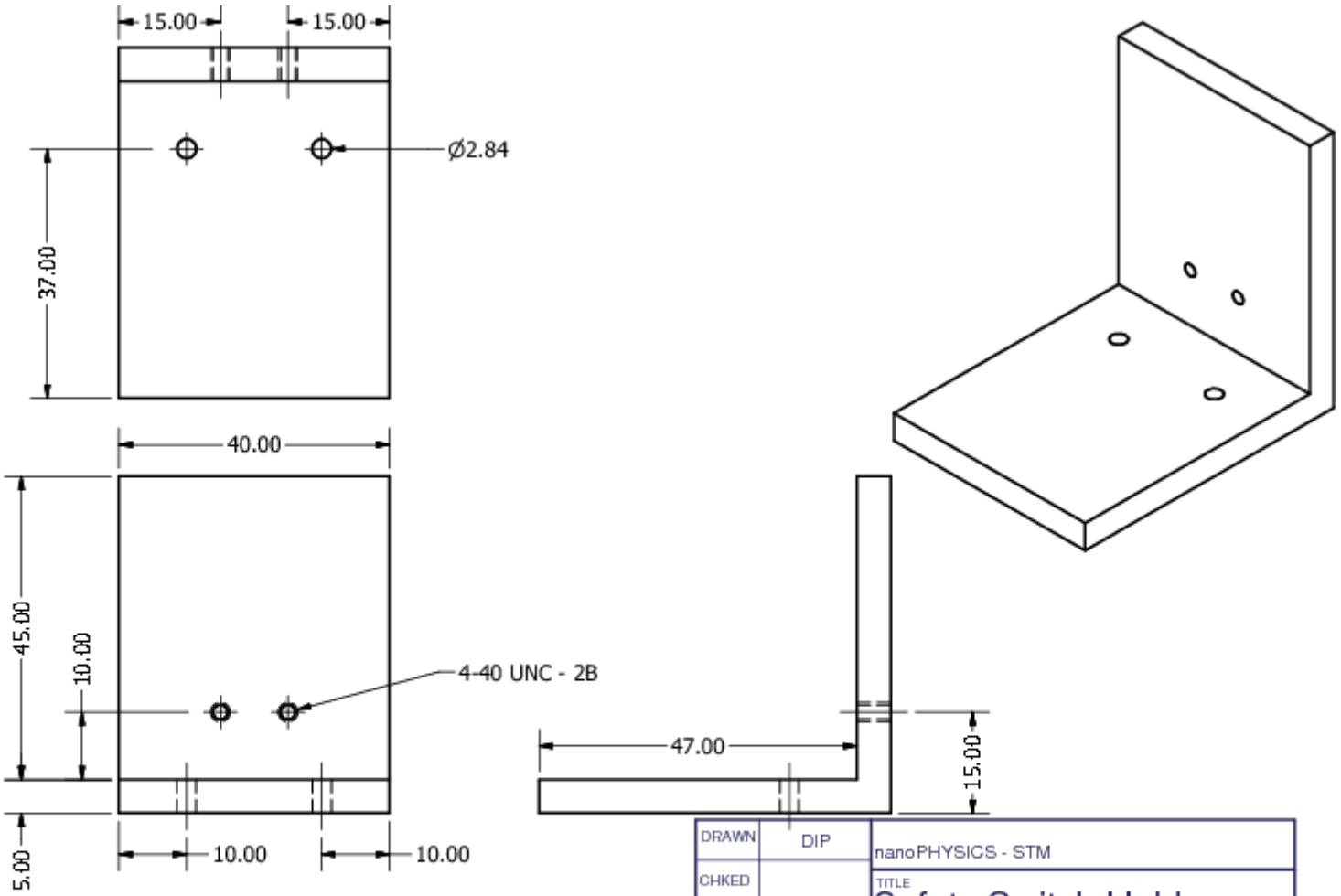

DRAWN	DIP	nanoPHYSICS - STM
CHKED		TITLE: Safety Switch Holder
SCALE	1:1	E:\Documents and Settings\nanoPhysics\My Documents\Inventor\Pendulum\Safety Switch Holder.idw
UNITS	mm	SPECIFIED: .X ±0.25, .XX ±0.15, .XXX ±0.03, ANG ± 1°
DATE	12/04/2010	DWG NO: Safety Switch Holder; REV
		MODEL: E:\Documents and Settings\nanoPhysics\My Documents\Inventor\Pendulum\Safety Switch Holder.ipt

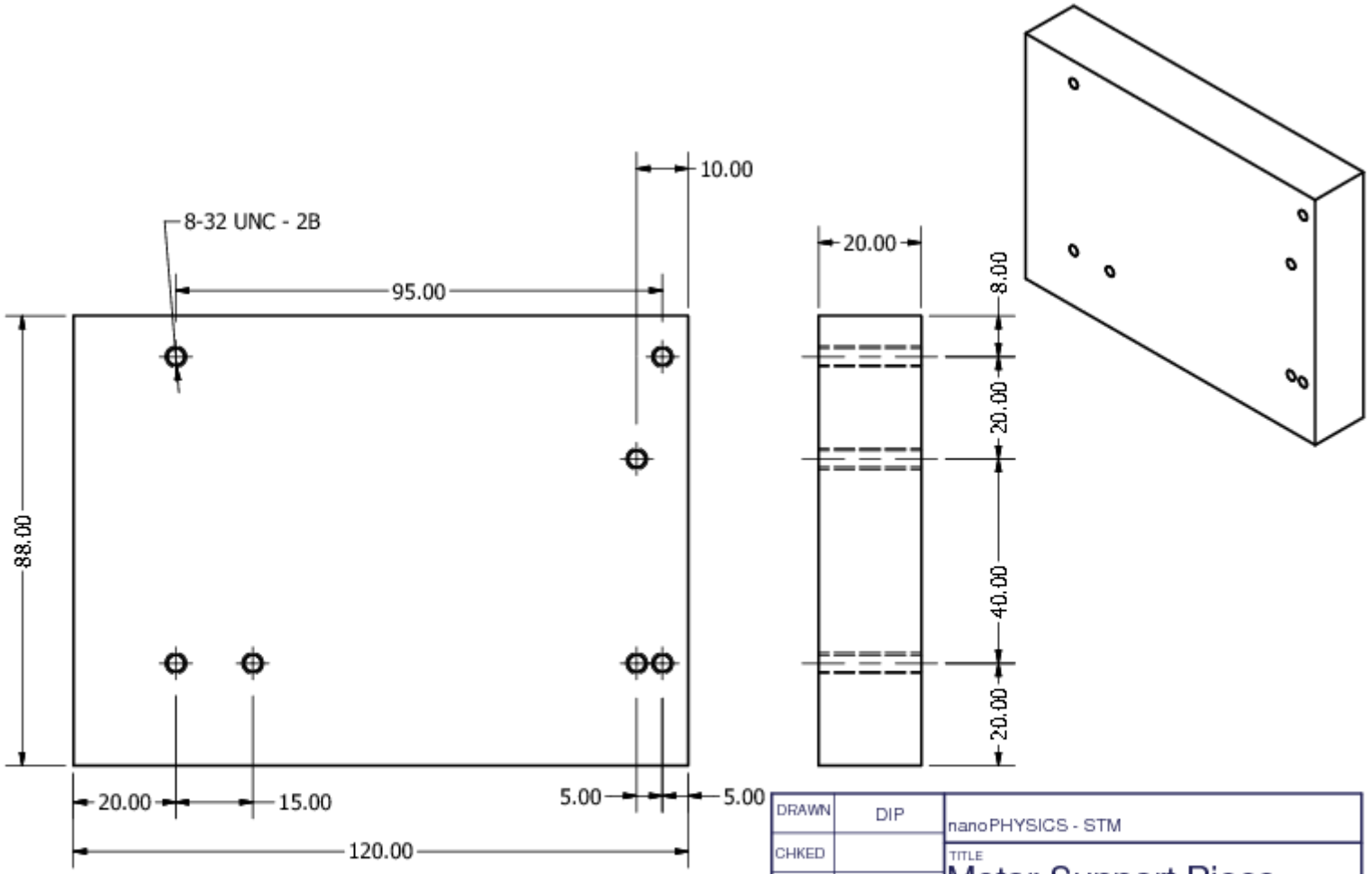

DRAWN	DIP
CHKED	
SCALE	1:1
UNITS	mm
DATE	12/04/2010

nanoPHYSICS - STM

TITLE

Motor Support Piece

E:\Documents and Settings\nanoPhysics\My Documents\Inventor\Pendulum\Motor Support.ipt

SPECIFIED:

.X	±0.25
.XX	±0.15
.XXX	±0.03
ANG	± 1°

DWG NO Motor Support

REV

MODEL: E:\Documents and Settings\nanoPhysics\My Documents\Inventor\Pendulum\Motor Support.ipt

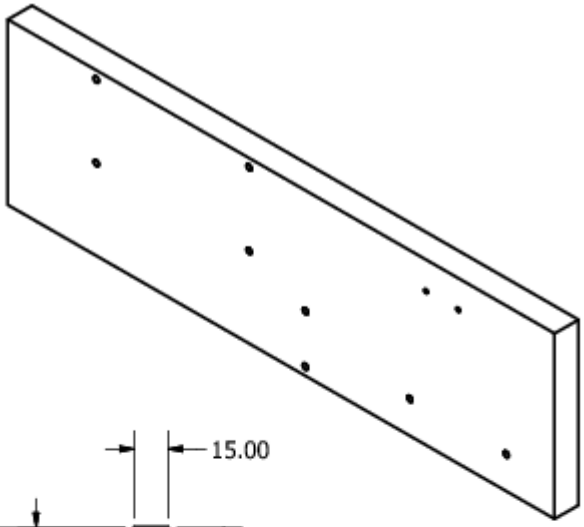

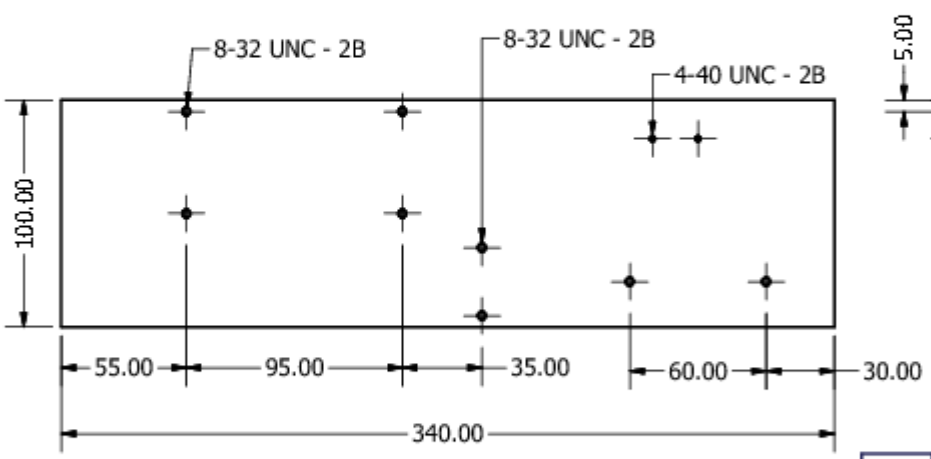

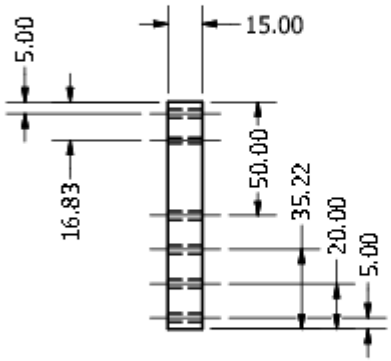

DRAWN	DIP	nanoPHYSICS - STM
CHKED		TITLE: Motor Base Plate
SCALE	1:1	E:\Program Files\Autodesk\Inventor 11\Templates\STM[mm].idw
UNITS	mm	UNLESS OTHERWISE SPECIFIED: .X ±0.25, .XX ±0.15, .XXX ±0.03, ANG ± 1° — MATERIAL — FINISH
DATE	12/04/2010	DWG NO — REV

MODEL: E:\Documents and Settings\nanoPhysics\My Documents\Inventor\Pendulum\Motor Base Plate.ipt

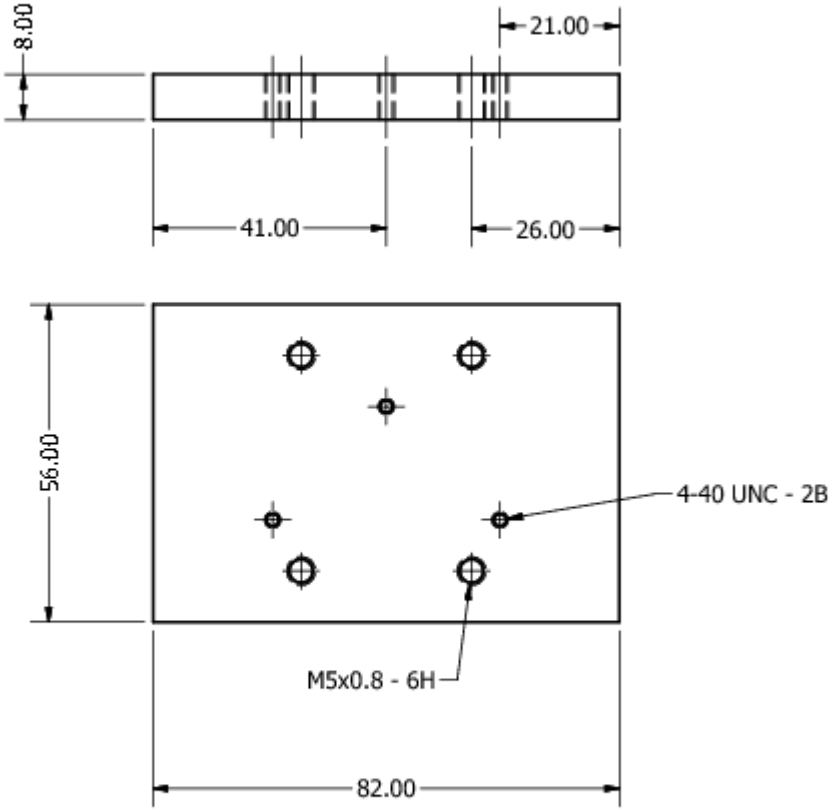

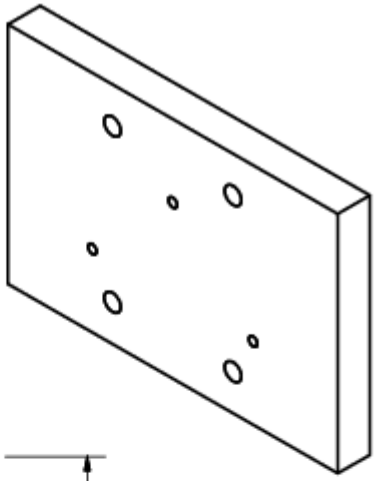

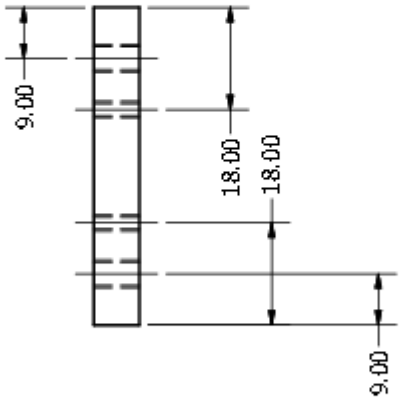

DRAWN	DIP	nanoPHYSICS - STM
CHKED		TITLE: Cart Base Plate
SCALE	1:1	E:\Documents and Settings\nanoPhysics\My Documents\Inventor\Pendulum\Cart Plate.idw
UNITS	mm	FINISH
DATE	12/04/2010	DWG NO: Cart Plate
		REV

SPECIFIED:
.X ±0.25
.XX ±0.15
.XXX ±0.03
ANG ± 1°

MODEL: E:\Documents and Settings\nanoPhysics\My Documents\Inventor\Pendulum\Cart Plate.ipt

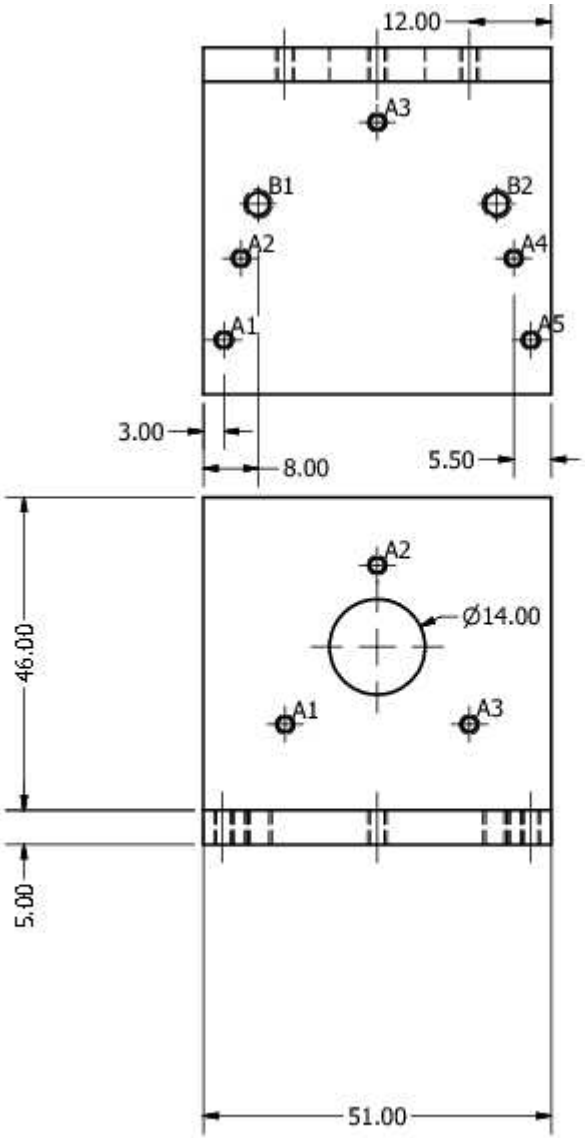

Hole Table	
HOLE	DESCRIPTION
A1	4-40 UNC - 2B
A2	4-40 UNC - 2B
A3	4-40 UNC - 2B
A4	4-40 UNC - 2B
A5	4-40 UNC - 2B
B1	8-32 UNC - 2B
B2	8-32 UNC - 2B

Hole Table	
HOLE	DESCRIPTION
A1	4-40 UNC - 2B
A2	4-40 UNC - 2B
A3	4-40 UNC - 2B

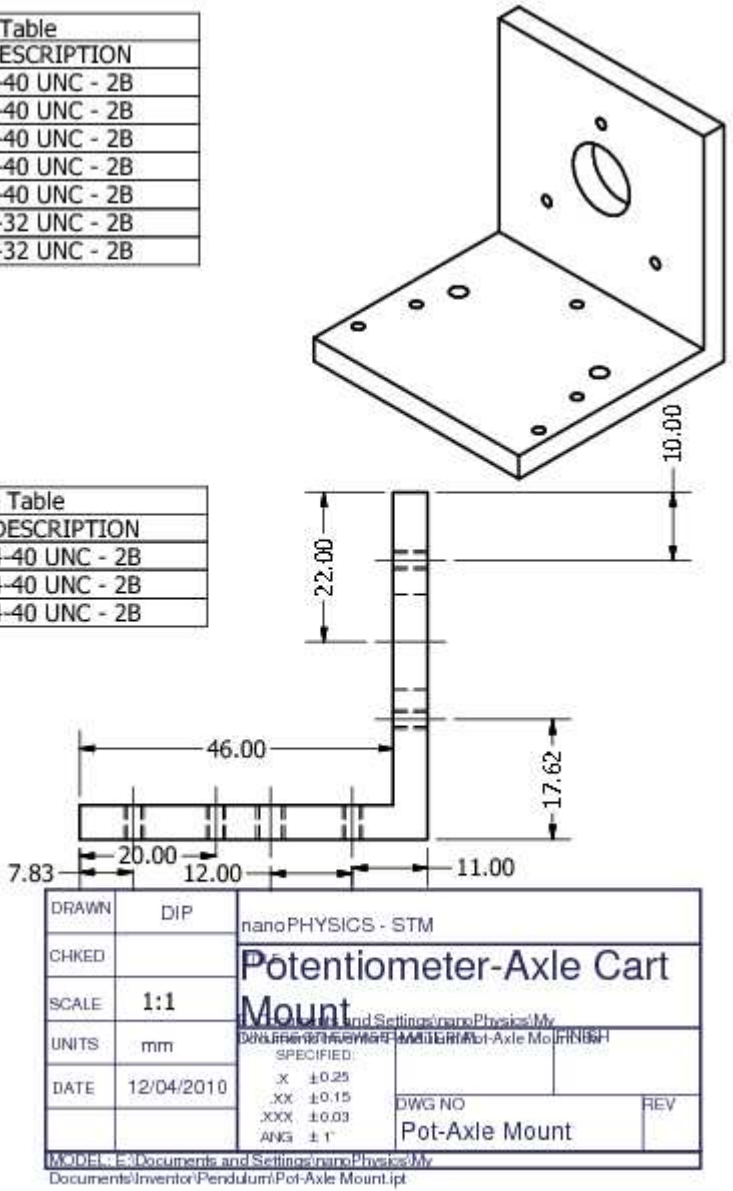

DRAWN	DIP
CHKED	
SCALE	1:1
UNITS	mm
DATE	12/04/2010

nanoPHYSICS - STM

Potentiometer-Axle Cart Mount

SPECIFIED:
.X ±0.25
.XX ±0.15
.XXX ±0.03
ANG ± 1°

DWG NO: Pot-Axle Mount

REV

MODEL: E:\Documents and Settings\nanoPhysics\My Documents\Inventor\Pendulum\Pot-Axle Mount.ipt

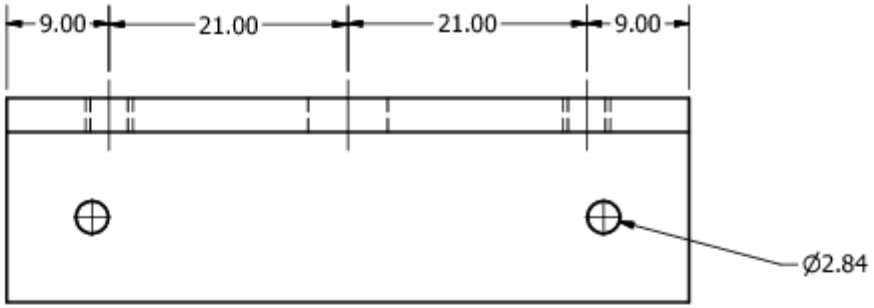

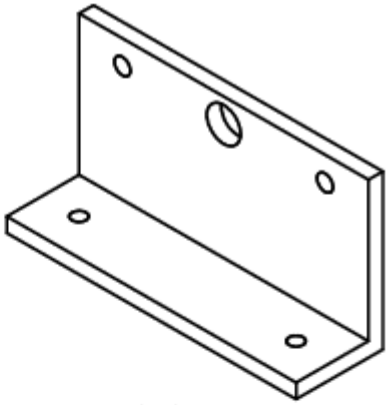

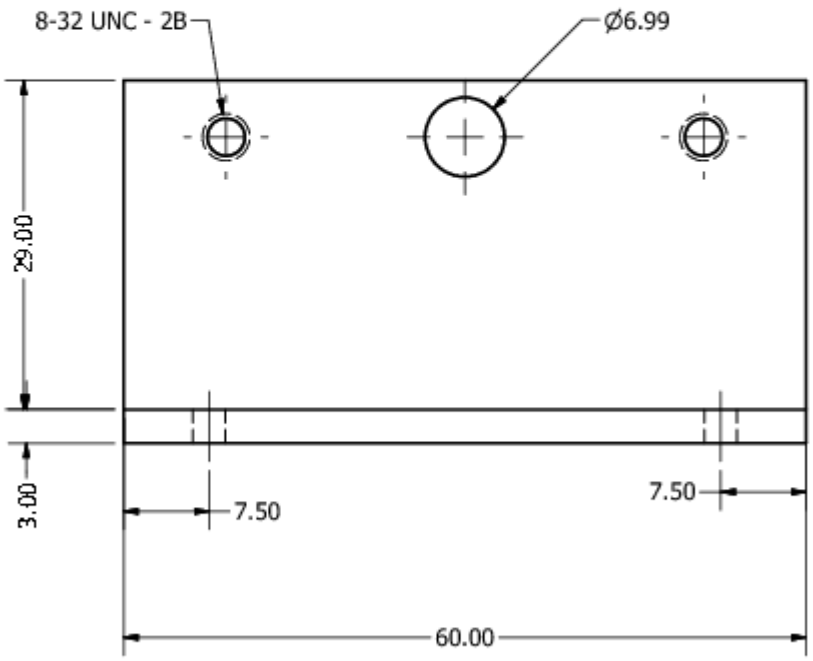

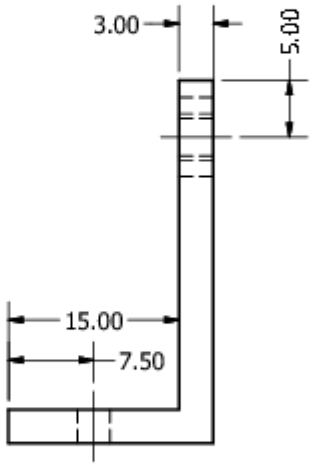

DRAWN	nanoPhysics	nanoPHYSICS - STM
CHKED		TITLE
SCALE	1:1	E:\Documents and Settings\nanoPhysics\My Documents\Inventor\Pendulum\Bearing Mount.ipt
UNITS	mm	FINISH
DATE	12/04/2010	SPECIFIED: .X ±0.25 .XX ±0.15 .XXX ±0.03 ANG ± 1°
		DWG NO Bearing Mount REV

MODEL: E:\Documents and Settings\nanoPhysics\My Documents\Inventor\Pendulum\Bearing Mount.ipt

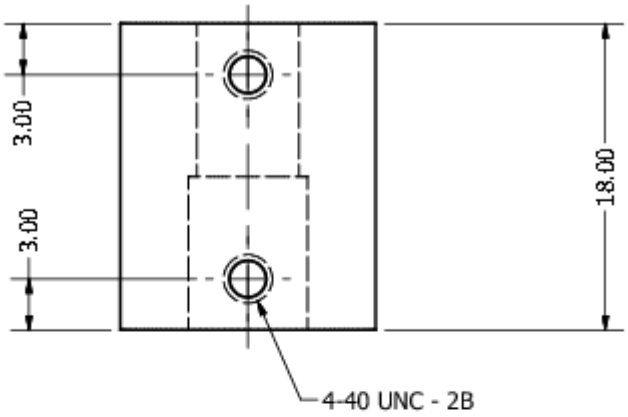

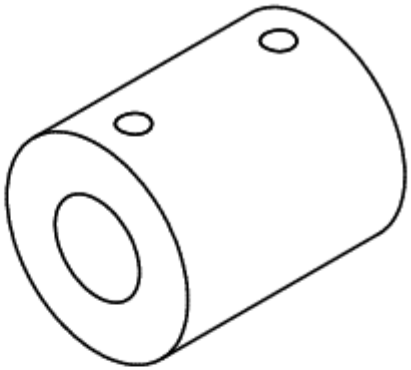

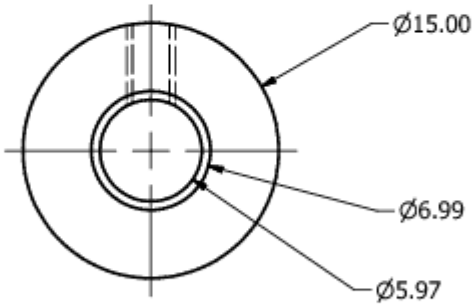

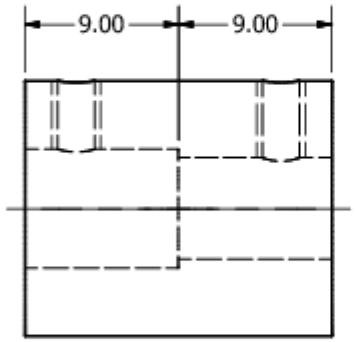

DRAWN	DIP	nanoPHYSICS - STM
CHKED		Axle-Potentiometer Shaft Coupler
SCALE	1:1	
UNITS	mm	
DATE	12/04/2010	

SPECIFIED:
.X ±0.25
.XX ±0.15
.XXX ±0.03
ANG ± 1°

DWG NO: AxlePot Shaft Coupler
REV:

MODEL: E:\Documents and Settings\nanoPhysics\My Documents\Inventor\Pendulum\AxlePot Shaft Coupler.ipt

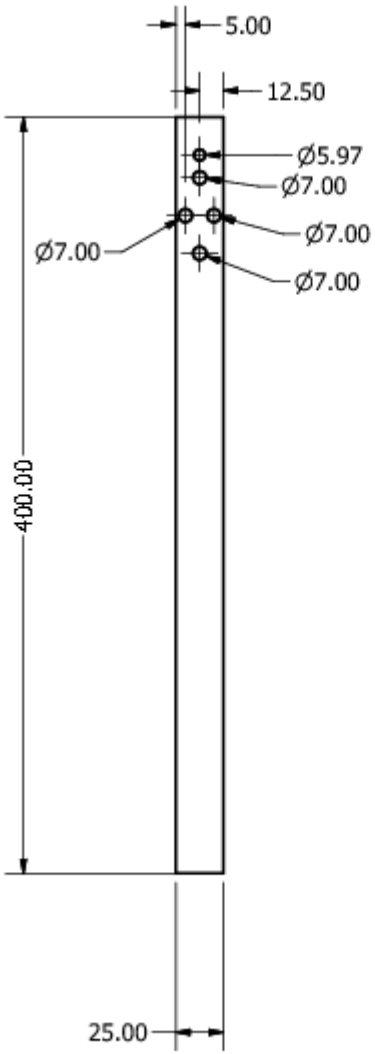

DRAWN	DIP	nanoPHYSICS - STM	
CHKED		TITLE: Link 2	
SCALE	1:1	E:\Documents and Settings\nanoPhysics\My Documents\Inventor\Pendulum\Link2.idw	FINISH
UNITS	mm	SPECIFIED: .X ±0.25 .XX ±0.15 .XXX ±0.03 ANG ± 1°	DWG NO: Link2
DATE	12/04/2010		REV
		MODEL: E:\Documents and Settings\nanoPhysics\My Documents\Inventor\Pendulum\Link2.ipt	

13 Appendix C - Safety Protocols

When Beginning Operation

- Inspect apparatus for damage and ensure all safety features are operational

During Operation

- No one is to stand in plane of pendulum during testing or operation
- Area around apparatus must be cleared of all objects
- No one is to directly touch apparatus when in operation except as necessary to operate

During Work on Apparatus

- Power to motors and sensors must be off when working on and around apparatus
- No one is to work alone when in lab or machine shop
- Machine shop safety rules must be followed

When Leaving Apparatus

- Ensure all power sources are off
- Ensure control program has exited

In Case of Injury

- Cut power to apparatus/machines in use
- Help injured person get medical attention if necessary
- Report injury to lab/machine shop supervisors once situation is under control

14 Appendix D - Task Breakdown

Will Beattie Treasurer

- Chief equipment procurer. Responsible for all orders.
- Lead communications officer. Responsible for all computer input/output procedures and sensor calibration.

Martin Esche Safety Officer

- Design and integration of home-made mechanical components.
- Assistant in construction of home-made mechanical components.

Andrew Fox Secretary

- Lead electrical engineer. Design and integration of additional analog electronics.
- Primary CAD specialist, responsible for generating relevant part drawings.

Peter Georgas Equipment Officer

- Lead in construction of mechanical components.
- Integration of sensors with mechanical components.

John Simpson Team Leader

- Lead control engineer. Responsible for flexible modeling and programming of control algorithms.

15 Appendix E - System Parameters & MATLAB Code

m_0	0.393 kg	Mass of cart
m_1	0.215 kg	Mass of first link
m_2	0.130 kg	Mass of second link
l_1	0.145 m	Distance from first revolute joint to first CM
l_2	0.134 m	Distance from second revolute joint to second CM
L_1	0.307 m	Pivot-to-pivot distance of first link
I_1	0.0032 kg m^2	CM moment of inertia of first link
I_2	0.0025 kg m^2	CM moment of inertia of second link
g	9.81 N/kg	Gravitational constant

```
function DoublePendulum

%-------------------------------------------------

%Set up analog input for pots
ai = analoginput('nidaq','Dev1');
inchan = addchannel(ai,[0,1,2],['Motor','T1','T2']); %Open Channel 1

set(ai,'SampleRate',10000)
set(ai,'SamplesPerTrigger',2);

%Set up analog output to BOP
ao = analogoutput('nidaq','Dev1');
outchan = addchannel(ao,1,'Output');
putsample(ao,0.0);
```

```
set(ao,'TriggerType','Manual');
set(ao,'TransferMode','Interrupts');


%-----------------------------------------------
%Define material parameters

g=9.81;
m0=0.393;  %Cart Mass
m1=.215;   %First Link Mass
m2=.130;   %Second Link mass
l1=.145;   %First link distance from pivot to CM
l2=0.134;   %Second link distance from pivot to CM
L1=0.307;   %Lengths of first pendulum from end to end
I1=(10/10)^2*m1*g*l1/4/pi^2 - m1*l1^2; %Calculate I_G1
I2=(5.28/5)^2*m2*g*l2/4/pi^2 - m2*l2^2;  %Calculate I_G2
cogradius=0.015;

%Define convenient parameters
d1 = m0+m1+m2;
d2 = m1*l1+m2*L1;
d3 = m2*l2;
d4 = m1*l1^2+m2*L1^2+I1;
d5 = m2*L1*l2;
d6 = m2*l2^2+I2;
f1 = (m1*l1+m2*L1)*g;
f2 = m2*l2*g;


%Build System Matricies
D = [d1,d2,d3;d2,d4,d5;d3,d5,d6];
iD = inv(D);
iDf = iD*[0,f1,f2]';
A = [0,0,0,1,0,0;
    0,0,0,0,1,0;
    0,0,0,0,0,1;
    0,iD(1,2)*f1,iD(1,3)*f2,0,0,0;
    0,iD(2,2)*f1,iD(2,3)*f2,0,0,0;
    0,iD(3,2)*f1,iD(3,3)*f2,0,0,0;
    ];
B = [0;0;0;iD*[1,0,0]'];
```

```
C = [1,0,0,0,0,0;
    0,1,0,0,0,0;
    0,0,1,0,0,0];
D=0;

%Create State Space System
sys = ss(A,B,C,D);

%Place Observer Gains
P = [-101,-100,-102,-103,-104,-105];
L = place(A',C',P)';

%Add integral state
Ai = [A,zeros(6,1);1,zeros(1,6)];
Bi = [B;0];

%Define LQR Weights
R = 2;
Q = [1/.001^2,0,0,0,0,0,0;  %x0
    0,1/.001^2,0,0,0,0,0; %t1
    0,0,1/.08^2,0,0,0,0; %t2
    0,0,0,1/3^2,0,0,0;   %x0dot
    0,0,0,0,1/.2^2,0,0;  %t1d0t
    0,0,0,0,0,1/.4^2,0; %t2dot
    0,0,0,0,0,0,1/.2^2]; %integral

%Calculate LQR Controller gains
[Ke,S,E] = lqr(Ai,Bi,Q,R);
K = Ke(1:6);
Ki = [Ke(7),0,0];


%Simulate System
T=0:0.01:20;
U=0.3*ones(size(T));
Ace = [A-B*K,B*K,-B*Ki;zeros(6,6),A-L*C,zeros(6,3);C,zeros(3,9)];
Bce = [zeros(1,12),-1,0,0]';
Cce = [C, zeros(size(C)),zeros(3,3)];
Dce = [0];
sys_cl = ss(Ace,Bce,Cce,Dce);
[Y,T,X]=lsim(sys_cl,U,T,[0,0,0,0,0,0,0,0,0,0,0,0,0,0,0,0,0,0]);
```

```
%Plotting
subplot(2,1,1)
 plot(T,X(:,1:3))
grid
 xlim([0,10])
hold on
legend('x','theta1', 'theta2')%, 'xd', 'td', 't2d')
plot(T,U,'--g');


xlabel('Time (s)','Interpreter','latex','FontSize',14,...
    'FontName','Arial');

ylabel('State Amplitude','Interpreter','latex',...
    'FontSize',14,...
    'FontName','Arial');

title('Step Response of Closed Loop DIP System',...
    'Interpreter','latex',...
    'FontSize',16,...
    'FontName','Arial');

%Fundamental Calibration Numbers
%AmpsPerVolt = 1.6352; %Martin's number
NMperAmp = 0.16;
AmpsPerVolt = 1.66; %My Number
coeff = cogradius/NMperAmp/AmpsPerVolt;


%Load Calibration
[V_Right,V_Left,V_Hang1,V_Invert1,V_Hang2,V_Invert2]=PotCalib;
poscal = .865/(V_Right-V_Left); %Convert voltage to position
anglecal1 = (pi-0)/(V_Hang1-V_Invert1); %Angle Calibration
anglecal2 = (pi-0)/(V_Hang2-V_Invert2); %Second Angle Calibration

%Initial variables
%expr=zeros(10000,11);

%Read initial positions
```

```
y = mean([getsample(ai);getsample(ai);getsample(ai);
    getsample(ai);getsample(ai);getsample(ai);getsample(ai)]);
y(1) = -.45 + poscal*(y(1)-V_Left);  %Convert Motor Pot to Position
y(2) = (0 + (y(2)-V_Invert1)*anglecal1);  %Convert Link Pot to Angle (radians)
y(2) = y(2); %THIS IS THE LINE WITH THE MINUS
y(3) = (0 + (y(3)-V_Invert2)*anglecal2);
y(3) = y(2)+y(3);
rad2deg(y)


xe=0; %Set integral state to zero
j=0; %Indexs saved data
t=0; %Time (i) variable
t_old = 0; %TIme (i-1) variable
stop=1; %Stopper variable
xhat = [y(1),y(2),y(3),0,0,0]';
%xhat = [-.05,0,0,0,0,0];
r=0; %Reference value for position

y=[0,0,0]; %Reset measurements

tic
while y(1) > -.45  && y(1) < .4 && abs(y(2)) < deg2rad(80),
    %While on the track, while pendulum hasn't fallen over

    %Read measurements
    y = mean([getsample(ai);getsample(ai);getsample(ai);
        getsample(ai);getsample(ai);getsample(ai);getsample(ai)]);
    y(1) = -.45 + poscal*(y(1)-V_Left);  \%Convert Motor Pot to Position
    y(2) = (0 + (y(2)-V_Invert1)*anglecal1);  \%Convert Link Pot to Angle (radians)
    y(2) = -.02 + y(2); \%THIS IS THE LINE WITH THE MINUS deg2rad(.2)
    y(3) = -.02 + (0 + (y(3)-V_Invert2)*anglecal2); \%deg2rad(.3)
    y(3) = y(2)+y(3);
    \%rad2deg(y)

    \%Calculate control force
    u = -K*xhat - Ke(7)*xe; \%Units of Force

    \%Scale control force to output voltage
    if(u > 0.1)
       output = (u+2.37)/2.9225;
```

```
    elseif(u < -.1)
       output = (u-2.0116)/2.4;
    else
        output = 0;
    end

    \%Set saturation limit
    if(abs(output) > 10)
        output = sign(output)*10;
    end

    \%Output voltage
    putsample(ao,output);

    \%Integrate forward control equations
    xhat = xhat + (t-t_old)*(A*xhat + B*u + L*(y'-C*xhat));
    xe = xe + (t-t_old)*(y(1)-r);

    \%Record data
    j=j+1;
    if(j<10001)
       expr(j,:)=[t,y,u,output,xhat'];
    else
       stop=1;
    end
    t_old=t;
    t=toc;
end

\%Set output to zero
putsample(ao,0.0);

\%Record Data
t = expr(:,1);
x0 = expr(:,2);
x1 = expr(:,3);
x2 = expr(:,4);

end
```

16 Appendix F - Theoretical Development

.

16.1 Derivation of System Equations

We let θ_0 denote the linear position of the cart along the track, relative to an arbitrary fixed reference, and we similarly denote the angular deviations of link 1 and link 2 from the vertical by θ_1 and θ_2. The cart and links have respective masses m_0, m_1 and m_2, and the links have center of mass moment of inertias I_1 and I_2. We denote the distance from the pivot of a respective link to its center of mass by l, and the pivot-to-pivot length by L. The variable u is a force applied to the cart in the positive θ_0 direction. It is this force we will use for our control procedure.

We use a Lagrangian approach to deriving the equations of motion for the cart. We first compute the kinetic energy of the system as

$$T = \frac{1}{2}\left[m_0||\boldsymbol{v_0}||^2 + m_1||\boldsymbol{v_1}||^2 + m_2||\boldsymbol{v_2}||^2\right] + \frac{1}{2}\left(I_{G_1}\dot{\theta_1}^2 + I_{G_2}\dot{\theta_2}^2\right)$$

where $||\cdot||$ denotes the Euclidian norm, $m_i \in \mathbb{R}$, $I_{G_i} \in \mathbb{R}$, and

$$\boldsymbol{v_0} = \frac{\mathrm{d}}{\mathrm{dt}}\boldsymbol{r}_0 = \frac{\mathrm{d}}{\mathrm{dt}}\left[\theta_0\hat{\boldsymbol{x}}\right]$$

$$\boldsymbol{v_1} = \frac{\mathrm{d}}{\mathrm{dt}}\boldsymbol{r}_1 = \frac{\mathrm{d}}{\mathrm{dt}}\left[(\theta_0 + l_1 sin\,\theta_1)\hat{\boldsymbol{x}} + (l_1 cos\,\theta_1)\hat{\boldsymbol{y}}\right]$$

$$\boldsymbol{v_2} = \frac{\mathrm{d}}{\mathrm{dt}}\boldsymbol{r}_2 = \frac{\mathrm{d}}{\mathrm{dt}}\left[(\theta_0 + L_1 \sin\,\theta_1 + l_2 \sin\,\theta_2)\hat{\boldsymbol{x}} + (L_1 cos\,\theta_1 + l_2 sin\,\theta_2)\hat{\boldsymbol{y}}\right]$$

The potential energy can be chosen to take the form

$$U = m_1 g l_1 cos\,\theta_1 + m_2 g(L_1 cos\,\theta_1 + l_2 \cos\,\theta_2)$$

with the final Lagrangian then being given by $\mathcal{L} = T - U$, namely

$$\begin{aligned}\mathcal{L} = & \frac{1}{2}\left(m_0 + m_1 + m_2\right)\dot{\theta}_0^2 \\ & + \frac{1}{2}(m_1 l_1^2 + m_2 L_1^2 + I_1)\dot{\theta}_1^2 + \frac{1}{2}(m_2 l_2^2 + I_2)\dot{\theta}_2^2 \\ & + (m_1 l_1 + m_2 L_1) cos(\theta_1)\dot{\theta}_0\dot{\theta}_1 \\ & + m_2 l_2 cos(\theta_2)\dot{\theta}_0\dot{\theta}_2 + m_2 L_1 l_1 cos(\theta_1 - \theta_2)\dot{\theta}_1\dot{\theta}_2 \\ & - (m_1 l_1 + m_2 L_1) g\, cos(\theta_1) - m_2 l_2 g\, cos(\theta_2)\end{aligned} \tag{2}$$

.

The Euler-Lagrange equations,

$$\frac{\mathrm{d}}{\mathrm{dt}}\left(\frac{\partial \mathcal{L}}{\partial \dot{\theta}_i}\right) - \frac{\partial \mathcal{L}}{\partial \theta_i} = u\delta_{0,i}$$

,

then yield the three nonlinear equations of motion for $i \in \{0, 1, 2\}$, given explicitly as

$$\Gamma = \left\{ \begin{array}{l} u = d_1\ddot{\theta}_0 + d_2\, cos(\theta_1)\ddot{\theta}_1 + d_3\, cos(\theta_2)\ddot{\theta}_2 - d_2\, sin(\theta_1)\dot{\theta}_1^2 - d_3\, sin(\theta_2)\dot{\theta}_2^2 \\ 0 = d_2\, cos(\theta_1)\ddot{\theta}_0 + d_4\ddot{\theta}_1 + d_5\, cos(\theta_1 - \theta_2)\ddot{\theta}_2 + d_5\, sin(\theta_1 - \theta_2)\dot{\theta}_2^2 - f_1\, sin(\theta_1) \\ 0 = d_3\, cos(\theta_2)\ddot{\theta}_0 + d_5\, cos(\theta_1 - \theta_2)\ddot{\theta}_1 + d_6\ddot{\theta}_2 - d_5 sin(\theta_1 - \theta_2)\dot{\theta}_1^2 - f_2\, sin(\theta_2) \end{array} \right\} \tag{3}$$

where the d_j and f_j depend only on physical system parameters and are defined in [Bogadanov, 2004].

16.2 Control Theory

The system Γ represents a highly nonlinear set of coupled differential equations. For our purposes, it is appropriate to work only within the linear regime defined by setting all positions and velocities equal to zero [1]. The linearizion of the system is accomplished by Taylor expanding each nonlinear term in each equation and retaining only terms to first order.

Under these conditions, one can recast the equations of motion in a standard form, referred to as a *Single-Input Multi-Output Linear Continuous-Time Invariant Control System*. To

[1] Note that the cart position can be set arbitrarily to zero, since it is a cyclic coordinate of $\mathcal{L}$

this end, we define the *state vector* of the system $\boldsymbol{x}(t) : \mathbb{R} \to \mathbb{R}^n$ as $\boldsymbol{x}(t) = [\theta_0\, \theta_1\, \theta_2\, \dot{\theta_0}\, \dot{\theta_1}\, \dot{\theta_2}]^T$. The linearized system can then be rearranged into the form

$$\dot{\boldsymbol{x}}(t) = \mathbf{A}\boldsymbol{x}(\boldsymbol{t}) + \boldsymbol{B}u(t) \tag{4}$$

where $\mathbf{A} \in \mathbb{R}^{6\times 6}$ and $B \in \mathbb{R}^{6\times 1}$ are matrices which depend only on the physical system parameters. This first order system is now amenable to a vast array of analysis techniques. The reader is referred to [Lewis, 2003] or [Astrom, 2008] for a detailed account of such techniques. We will simply make use of the results without justification.

A useful concept for us is that of *controllability*. Intuitively, controllability refers to our ability to access all of the system states using our input. For example, if one of the equations is completely decoupled from the input, we will obviously have no way to access and influence it, and it will evolve according to its own (possibly unstable) dynamics in spite of our actions. One can show that if the controllability matrix, defined as

$$C(A, B) = [B \mid b \mid A^2B \mid \cdots \mid A^5B]$$

is nonsingular, we are guaranteed that the (quite unstable) linearized system can be stabilized by a state feedback law of the form $u(t) = -K^T\boldsymbol{x}(t)$ for $K \in \mathbb{R}^{6\times 1}$. We note that this is not simply "proportional control" as is common in PID controllers.

Equation 4 then becomes

$$\dot{\boldsymbol{x}}(t) = (A - BK^T)\boldsymbol{x}(t)$$

One can show that the stability of the closed loop system then depends on the eigenvalues of $A - BK^T$. If $\text{spec}(A - BK^T) \subset \mathbb{C}^-$, we will have exponential decay of all states to zero, and hence, upright stability. The well known *pole placement* theorem guarantees that we can in turn choose a K that will accomplish this [2]. A discussion revolving around the choice of K can be found in the main report.

It is clear that the control procedure developed requires we have full knowledge of $\boldsymbol{x}(t)$ at all times. When faced with the issue of measurement, we must recognize that we cannot measure all of the state variables. We instead have access only to an output vector $\boldsymbol{y} \in \mathbb{R}^p$, $\boldsymbol{y} = C\boldsymbol{x}$ for some $n \times p$ matrix C. A useful concept in this case is that of *observability*. Intuitively, this refers to how good a look we can get at the state $\boldsymbol{x}$ from simply observing

[2] Specifically, the pole placement theorem guarantees that we can assign an arbitrary real, monic polynomial to the characteristic polynomial of $A - BK^T$.

the output $\boldsymbol{y}$. For example, consider an Op-Amp adder system, adding two voltages V_1 and V_2 to produce V_out. We clearly will not be able to determine the time evolution of both the input voltages simply from the output. It turns out that if the *observability* matrix $O(A, C)$, defined as

$$\boldsymbol{O(A, C)} = \begin{bmatrix} \boldsymbol{C} \\ \boldsymbol{CA} \\ \vdots \\ \boldsymbol{CA}^{n-1} \end{bmatrix}$$

is nonsingular, we can create a *state observer* which infers the full state from the vector $\boldsymbol{y}$. We need to get a bit creative here. Consider an estimated value of $\boldsymbol{x}$, $\hat{\boldsymbol{x}}$, whose dynamics are governed by

$$\frac{\mathrm{d}}{\mathrm{dt}}\hat{\boldsymbol{x}} = A\hat{\boldsymbol{x}} + Bu + L(\boldsymbol{y} - C\hat{\boldsymbol{x}})$$

.

for some nonsingular matrix L of our choosing. Subtracting Equation 4 from this, we find that the state error, $\boldsymbol{e} = \hat{\boldsymbol{x}} - \boldsymbol{x}$ is governed by

$$\dot{\boldsymbol{e}} = (A - LC)\boldsymbol{e}$$

.

An appropriate choice of L will then guarantee that our estimated state vector converges asymptotically to the true state. Note that we are free to choose L however we wish, and are not confined by physical saturation of actuators or sensors. In the absence of an advanced real-time filtering system to numerically differentiate the position measurements to obtain velocities, this method provides an accurate way of estimating the full state.

In order to control the position of the cart, we introduce an *integral state* defined by $\dot{x}_i = \theta_0 - r$ for a reference position r of our choosing. This integral state will function much like integral gain does in a PID controller, driving the system to the reference point and producing zero steady-state error. Note that we can now simply recast our controller as $u(t) = -K^T\boldsymbol{x}(t) - K_i x_i = -K'\boldsymbol{x}'(t)$ for an extended state vector $\boldsymbol{x}'(t)$.

References

Murray R.M. Astrom, K.J. *Feedback Systems: An Introduction fir Scientists and Engineers.* Princeton University Press, 2008.

A. Bogadanov. Optimal control of a double inverted pendulum on a cart. *CSE*, 04(006), 2004.

Shao J. Bradshaw, A. Swing-up control of inverted pendulum systems. *Robotica*, 14: 397–405, 1996.

Jehandad Khan, Khalid Munawar, Raja Amer Azeem, and Muhammad Salman. Inverted pendulum with moving reference for benchmarking control systems performance. In *ACC'09: Proceedings of the 2009 conference on American Control Conference*, pages 3764–3768, Piscataway, NJ, USA, 2009. IEEE Press. ISBN 978-1-4244-4523-3.

A. Lewis. *An Introduction to Mathematical Control Theory.* Unpublished, 2003.

Ying Wang, Zhixian Lin, and Maoqing Li. Sampled-data observer for inverted-pendulum with large sampling interval. *Computer Modeling and Simulation, International Conference on*, 1:59–62, 2010. doi: http://doi.ieeecomputersociety.org/10.1109/ICCMS.2010.31.